



CHORUS

This is the accepted manuscript made available via CHORUS. The article has been published as:

Phenomenology of a supersymmetric $U(1)_{\{B-L\}} \times U(1)_{\{R\}}$ extension of the standard model with inverse seesaw mechanism

M. Hirsch, L. Reichert, W. Porod, and F. Staub

Phys. Rev. D **86**, 093018 — Published 16 November 2012

DOI: [10.1103/PhysRevD.86.093018](https://doi.org/10.1103/PhysRevD.86.093018)

Phenomenology of a supersymmetric $U(1)_{B-L} \times U(1)_R$ extension of the standard model with inverse seesaw mechanism

M. Hirsch* and L. Reichert†

*AHEP Group, Instituto de Física Corpuscular – C.S.I.C./Universitat de València
Edificio de Institutos de Paterna, Apartado 22085, E-46071 València, Spain*

W. Porod‡

*Institut für Theoretische Physik und Astronomie, Universität Würzburg
Am Hubland, 97074 Würzburg
AHEP Group, Instituto de Física Corpuscular – C.S.I.C./Universitat de València
Edificio de Institutos de Paterna, Apartado 22085, E-46071 València, Spain*

F. Staub§

*Bethe Center for Theoretical Physics & Physikalisches Institut der Universität Bonn,
Nussallee 12, 53115 Bonn, Germany*

Abstract

We discuss the minimal supersymmetric $U(1)_{B-L} \times U(1)_R$ extension of the standard model. Gauge couplings unify as in the MSSM, even if the scale of $U(1)_{B-L} \times U(1)_R$ breaking is as low as order TeV and the model can be embedded into an $SO(10)$ grand unified theory. The phenomenology of the model differs in some important aspects from the MSSM, leading potentially to rich phenomenology at the LHC. It predicts more light Higgs states and the mostly left CP-even Higgs has a mass reaching easily 125 GeV, with no constraints on the SUSY spectrum. Right sneutrinos can be the lightest supersymmetric particle, changing all dark matter constraints on SUSY parameter space. The model has seven neutralinos and squark/gluino decay chains involve more complicated cascades than in the MSSM. We also discuss briefly low-energy and accelerator constraints on the model, where the most important limits come from recent Z' searches at the LHC and upper limits on lepton flavour violation.

PACS numbers: 14.60.Pq, 12.60.Jv, 14.80.Cp

Keywords: supersymmetry; neutrino masses and mixing; LHC

*Electronic address: mahirsch@ific.uv.es

†Electronic address: reichert@ific.uv.es

‡Electronic address: porod@physik.uni-wuerzburg.de

§Electronic address: fnstau@th.physik.uni-bonn.de

I. INTRODUCTION

Within the minimal supersymmetric extension of the standard model (MSSM) the gauge couplings unify nearly perfectly around an energy scale of approximately $m_G \simeq 2 \times 10^{16}$ GeV, if SUSY particles exist with masses of the order of $\mathcal{O}(1)$ TeV. Extending the MSSM with non-singlet superfields tends to destroy this attractive feature, unless (a) the additional fields come in complete $SU(5)$ multiplets or (b) the standard model gauge group is extended too. Here we study a model in which the SM group is enlarged to $SU(3)_c \times SU(2)_L \times U(1)_{B-L} \times U(1)_R$. It is a variant of the models first proposed in [1] and later discussed in more detail in [2].

Our main motivation for studying this model can be summarized as: (i) It unifies, in the same way the MSSM does, even if the scale of $U(1)_{B-L} \times U(1)_R$ breaking is as low as the electro-weak scale; (ii) it can be easily embedded into an $SO(10)$ grand unified theory; (iii) it has the right ingredients to explain neutrino masses (and angles) by either an inverse [3] or a linear [4, 5] seesaw; (iv) it allows for Higgs masses significantly larger than the MSSM without the need for a very heavy SUSY spectrum [6] and (v) it potentially leads to rich phenomenology at the LHC.

With the data accumulated in 2011 both ATLAS [7] and CMS [8] have seen some indications for a Higgs boson with a mass of roughly $m_h \sim 125$ GeV. This result, perhaps unsurprisingly, has triggered an avalanche of papers studying the impact of such a relatively hefty Higgs on the supersymmetric parameter space [9–43]. The general consensus seems to be, that the MSSM can generate $m_h \sim 125$ GeV only if squarks and gluinos have masses in the multi-TeV range. While this is, of course, perfectly consistent with the lower bounds on SUSY masses obtained from \cancel{E}_T searches at the LHC [44, 45], such a heavy spectrum could make it quite difficult indeed for the LHC to find direct signals for SUSY.

There are, of course, several possibilities to circumvent this conclusion. First of all, it is well-known that the loop corrections to h^0 are dominated by the top quark-squark loops. Thus, little or no constraints on sleptons and on squarks of the first two generations can in fact be derived from Higgs mass measurements, once the assumption of universal boundary conditions for the soft SUSY parameters is abandoned. Second, in the next-to-minimal SSM (NMSSM) the h^0 can be heavier than in the MSSM due to the presence of new F-terms from the additional singlet Higgs [18, 43], especially in models with non-universal boundary conditions for the (soft) Higgs mass terms [25] or in the generalized NMSSM [26, 27]. And, third, in models with an extended gauge group additional D -terms contribute to the Higgs mass matrices, relaxing the MSSM upper limit considerably [46–50]. This latter possibility is the case we have studied in a previous paper [6] using the minimal $U(1)_{B-L} \times U(1)_R$ models of [1]. Here, we extend the analysis of [6], including both Higgs and SUSY phenomenology.

Due to the extended gauge structure the model necessarily has more Higgses than the MSSM. Near D-flatness of the $U(1)_{B-L} \times U(1)_R$ breaking then results in one additional light Higgs, h_{BLR}^0 [6]. Mixing between the MSSM $h^0 \equiv h_L^0$ and h_{BLR}^0 enhances the mass of the mostly MSSM Higgs and, potentially, affects its decays. This is reminiscent to the

situation in the NMSSM, where an additional light and mostly singlet Higgs state seems to be preferred [18, 43] if the signals found by ATLAS [7] and CMS [8] are indeed due to a 125 GeV Higgs.

The MSSM-like h_L^0 in our model can have some exotic decays. For example, the h_L^0 will decay to two lighter Higgses, if kinematically possible, although this decay can never be dominant due to constraints coming from LEP. The model also includes right-handed neutrinos with electro-weak scale masses and there is a small but interesting part in parameter space where $m_{Z^0} \leq m_{\nu_R} \leq m_{h_L^0}$, where the Higgs decays to two neutrinos. These decays always lead to one light and one heavy neutrino, with the latter decaying promptly to either $W^\pm l^\mp$ or $Z^0 \nu$. (Mostly right) sneutrinos can be lighter than the h_L^0 , in which case the Higgs can have invisible decays.

The SUSY spectrum of the model is also richer than the MSSM: It has seven neutralinos and nine sneutrino states. These additional sneutrinos can easily be the lightest supersymmetric particle (LSP) and thus change all the constraints on SUSY parameter space, usually derived from the requirement that the neutralino be a good dark matter candidate with the correct relic density [51]¹. Even though the lightest sneutrino can also be the LSP in the MSSM, direct detection experiments have ruled out this possibility a long time ago [52]. In SUSY decays, within the MSSM right squarks decay directly to the bino-like neutralino, leading to the standard missing momentum signature of supersymmetry. Due to the extended gauge group, right squarks can decay also to heavier neutralinos, leading to longer decay chains and potentially to multiple lepton edges². Decays of the heavier neutralinos also produce Higgses, both the h_L^0 and the h_{BLR}^0 appear, with ratios depending on the right higgsino content of the neutralinos in the decay chains.

The rest of this paper is organized as follows. In the next section we discuss the setup of the model, its particle content, superpotential and soft terms and the symmetry breaking. The phenomenologically most interesting mass matrices of the spectrum are given in section III where we also discuss numerical results on the SUSY and Higgs mass eigenstates. Here, we focus on Higgs and slepton/sneutrino masses, which are the phenomenologically most interesting. In section IV we define some benchmark points for the model and discuss their phenomenologically most interesting decay chains. We then close with a short summary. In the appendix we give mass matrices not presented in the text, formulas for the 1-loop corrections in the Higgs sector and more information about the calculation of the RGEs, including anomalous dimensions as well as the 1-loop β functions for gauge couplings and gauginos.

¹ Also for the case of a neutralino LSP, constraints on the SUSY parameter space from dark matter can change in case the right Higgsino is light.

² Longer SUSY cascades from larger number of neutralino states have also been discussed in [53, 54].

	Superfield	$SU(3)_c \times SU(2)_L \times U(1)_R \times U(1)_{B-L}$	Generations
	\hat{Q}	$(\mathbf{3}, \mathbf{2}, 0, +\frac{1}{6})$	3
	\hat{d}^c	$(\bar{\mathbf{3}}, \mathbf{1}, +\frac{1}{2}, -\frac{1}{6})$	3
	\hat{u}^c	$(\bar{\mathbf{3}}, \mathbf{1}, -\frac{1}{2}, -\frac{1}{6})$	3
	\hat{L}	$(\mathbf{1}, \mathbf{2}, 0, -\frac{1}{2})$	3
	\hat{e}^c	$(\mathbf{1}, \mathbf{1}, +\frac{1}{2}, +\frac{1}{2})$	3
	$\hat{\nu}^c$	$(\mathbf{1}, \mathbf{1}, -\frac{1}{2}, +\frac{1}{2})$	3
	\hat{S}	$(\mathbf{1}, \mathbf{1}, 0, 0)$	3
	\hat{H}_u	$(\mathbf{1}, \mathbf{2}, +\frac{1}{2}, 0)$	1
	\hat{H}_d	$(\mathbf{1}, \mathbf{2}, -\frac{1}{2}, 0)$	1
	$\hat{\chi}_R$	$(\mathbf{1}, \mathbf{1}, +\frac{1}{2}, -\frac{1}{2})$	1
	$\hat{\bar{\chi}}_R$	$(\mathbf{1}, \mathbf{1}, -\frac{1}{2}, +\frac{1}{2})$	1

TABLE I: The Matter and Higgs sector field content of the $U(1)_R \times U(1)_{B-L}$ model. Generation indices have been suppressed. The \hat{S} superfields are included to generate neutrino masses via the inverse seesaw mechanism. Under matter parity, the matter fields are odd while the Higgses are even.

II. THE MODEL: $SU(3)_c \times SU(2)_L \times U(1)_{B-L} \times U(1)_R$

In this section we present the particle content of the model, its superpotential and discuss the symmetry breaking. We consider the simplest model based on the gauge group $SU(3)_c \times SU(2)_L \times U(1)_R \times U(1)_{B-L}$. We will call this the mBLR model below. As has been shown in [1] it can emerge as the low-energy limit of a certain class of $SO(10)$ GUTs broken along the “minimal” left-right symmetric chain [55, 56]

$$\begin{aligned}
SO(10) &\rightarrow SU(3)_c \times SU(2)_L \times SU(2)_R \times U(1)_{B-L} \\
&\rightarrow SU(3)_c \times SU(2)_L \times U(1)_R \times U(1)_{B-L}.
\end{aligned} \tag{1}$$

The main virtue of this setting is that an MSSM-like gauge coupling unification is achieved with a sliding $U(1)_R \times U(1)_{B-L}$ breaking scale, i.e. this last stage can stretch down even to the electro-weak scale. Different from the previous works [1, 2], we assume that the first two breaking steps down to $U(1)_R \times U(1)_{B-L}$ happen both at (or sufficiently close to) the GUT scale. This assumption is used only for simplifying our setup, it does not lead to any interesting changes in phenomenology.

A. Particle content, superpotential and soft terms

The transformation properties of all matter and Higgs superfields of the model are summarized in table I. Apart from the MSSM fields, in the matter sector we have $\hat{\nu}^c$ and \hat{S} .

The former are necessary in the extended gauge group for anomaly cancellation,³ while the fields \hat{S} are included to explain neutrino masses by either an inverse [3] or a linear [4, 5] seesaw mechanism. Our Higgs sector, including the new fields $\hat{\chi}_R$ and $\hat{\bar{\chi}}_R$, is the minimal one for the breaking of $U(1)_{B-L} \times U(1)_R$ to $U(1)_{EM}$.

The fields χ_R and $\bar{\chi}_R$ can be viewed as the (electric charge neutral) remnants of $SU(2)_R$ doublets, which remain light in the spectrum when the $SU(2)_R$ gauge factor is broken by the vev of a $B-L$ neutral triplet down to the $U(1)_R$ [1]. The presence of $\hat{\chi}_R$ and $\hat{\bar{\chi}}_R$ makes it necessary to introduce an extra Z_2^M matter parity, since otherwise R -parity is broken in a potentially disastrous way, once these scalars acquire vacuum expectation values. This Z_2^M is not a particular feature of our setup; it is always needed in models where $U(1)_{B-L}$ is broken with doublets [57].⁴

Models with a sliding $U(1)_R \times U(1)_{B-L}$ scale and $(B-L)$ -even Higgses can be constructed as well. These would simply require that the fields $\hat{\chi}_R$ (and its partner) are replaced by fields which transform as $(1, 1, 1/2, \pm 1)$. These can be understood as the neutral components of $SU(2)_R$ triplets, remaining light in the spectrum when $SU(2)_R$ is broken to $U(1)_R$. Such a construction has the advantage that R -parity is automatically conserved, different from the model we study here, which needs the introduction of matter parity to guarantee the stability of the LSP. However, the disadvantage of these models is that they necessarily lead to a type-I seesaw instead of an inverse seesaw. Note that such a low-scale type-I seesaw would overshoot experimental bounds on neutrino masses, unless the neutrino Yukawa couplings are assumed to be tiny, $\mathcal{O}(10^{-6})$ or smaller.⁵

For the particle content of table I the relevant R -parity and Z_2^M conserving superpotential is given by

$$W = W_{\text{MSSM}} + W_S. \quad (2)$$

Here,

$$\begin{aligned} W_{\text{MSSM}} &= Y_u \hat{u}^c \hat{Q} \hat{H}_u - Y_d \hat{d}^c \hat{Q} \hat{H}_d - Y_e \hat{e}^c \hat{L} \hat{H}_d + \mu \hat{H}_u \hat{H}_d \\ W_S &= Y_\nu \hat{\nu}^c \hat{L} \hat{H}_u + Y_s \hat{\nu}^c \hat{\chi}_R \hat{S} - \mu_R \hat{\chi}_R \hat{\chi}_R + \mu_S \hat{S} \hat{S}. \end{aligned} \quad (3)$$

where Y_e , Y_d and Y_u are the usual MSSM Yukawa couplings for the charged leptons and the quarks. In addition there are the neutrino Yukawa couplings Y_ν and Y_s ; the latter mixes the ν^c fields with the S fields giving rise to heavy SM-singlet pseudo-Dirac mass eigenstates. The term μ_R is completely analogous to the MSSM μ term. Note that the term μ_S is included to generate non-zero neutrino mass with an inverse seesaw mechanism. However, as always is done in inverse seesaw, we assume that μ_S is much smaller than all other dimensionful parameters of the model. Apart from neutrino masses themselves it will therefore not affect any of the mass matrices (or decays) of our interest.

³ $\hat{\nu}^c$ is automatically part of the theory due to its $SO(10)$ origin.

⁴ In the normalization of [57] doublets have $U(1)_{B-L} = 1$, i.e are “odd” under B-L.

⁵ For discussion of R -parity in LR-models see [58–60].

Note that, besides the role it plays in neutrino physics, the Y_s coupling is relevant also for the Higgs phenomenology at the loop level as it enters the mixing of χ_R and $\bar{\chi}_R$ Higgs fields with the $SU(2)_L$ Higgs doublets as well as the RGEs for χ_R , see below.

Following the notation and conventions of [61] the soft SUSY breaking Lagrangian reads

$$V_{soft} = \sum_{ij} m_{ij}^2 \phi_i^* \phi_j + \left(\sum_a M_a \lambda_a \lambda_a + T_u \tilde{u}_R^* \tilde{Q} H_u - T_d \tilde{d}_R^* \tilde{Q} H_d + T_\nu \tilde{\nu}_R^* \tilde{L} H_u - T_e \tilde{e}_R^* \tilde{L} H_d + B_\mu H_u H_d - B_{\mu_R} \bar{\chi}_R \chi_R + T_s \tilde{\nu}_R^* \chi_R \tilde{S} + B_{\mu_S} \tilde{S} \tilde{S} + h.c. \right). \quad (4)$$

The first sum contains the scalar masses squared and the second sum runs over all gauginos for the different gauge groups (called λ_{BL} , λ_R , λ_L^i and λ_G^α in the following) and the second one contains the scalar masses squared. While B_{μ_S} is in principle a free parameter, a naive order of magnitude expectation for it is $B_{\mu_S} \sim \mu_S m_{SUSY}$. Thus, one expects that B_{μ_S} is much smaller than all other soft terms and can be safely neglected, see discussion of sneutrinos below.

To reduce the number of free parameters, in our numerical studies we will consider a scenario motivated by minimal supergravity. This means that we assume a GUT unification of all soft-breaking sfermion masses as well as a unification of all gaugino mass parameters

$$m_0^2 \delta_{ij} = m_D^2 \delta_{ij} = m_U^2 \delta_{ij} = m_Q^2 \delta_{ij} = m_E^2 \delta_{ij} = m_L^2 \delta_{ij} = m_{\nu^c}^2 \delta_{ij} \quad (5)$$

$$M_{1/2} = M_{BL} = M_R = M_2 = M_3$$

Also, for the trilinear soft-breaking coupling, the ordinary mSugra conditions are assumed

$$T_i = A_0 Y_i, \quad i = e, d, u, \nu, s. \quad (6)$$

The GUT scale is chosen as the unification scale of g_{BL} , g_R and g_L , while we allow g_3 to be slightly different, exactly as in the MSSM. A complete unification is assumed to happen due to GUT threshold corrections. For the remaining soft parameters in the Higgs sector, $m_{H_d}^2$, $m_{H_u}^2$, $m_{\chi_R}^2$, $m_{\bar{\chi}_R}^2$ and μ , B_μ , μ_R and B_{μ_R} , we have implemented two different options. These are discussed in section II B.

The presence of two Abelian groups gives rise to gauge kinetic mixing

$$-\chi_{ab} \hat{F}^{B-L, \mu\nu} \hat{F}_{\mu\nu}^R. \quad (7)$$

This is allowed by gauge and Lorentz invariance [62], as $\hat{F}^{B-L, \mu\nu}$ and $\hat{F}^{R, \mu\nu}$ are gauge invariant, see e.g. [63]. Even if $U(1)_R$ and $U(1)_{B-L}$ are orthogonal in $SO(10)$ the kinetic mixing term will be induced during the RGE running below the $SU(2)_R$ breaking scale because the light fields remaining below the GUT scale can't be arranged in complete $SO(10)$ multiplets: while all matter fields form three generations of 16-plets, $\hat{\chi}_R$ and $\hat{\bar{\chi}}_R$ induce off-diagonal elements already in the 1-loop matrix of the anomalous dimensions defined by $\gamma_{RBL} = \frac{1}{16\pi^2} \text{Tr} Q_R Q_{B-L}$. The matrix reads

$$\gamma = \frac{1}{16\pi^2} N \begin{pmatrix} \frac{15}{2} & -\frac{1}{2} \\ -\frac{1}{2} & \frac{9}{2} \end{pmatrix} N. \quad (8)$$

$N = \text{diag}(1, \sqrt{\frac{3}{2}})$ contains the GUT normalization of the two Abelian gauge groups. Our implementation follows the description of [64], where it is shown that terms of the form as in eq. (7) can be absorbed in the covariant derivative by a re-definition of the gauge fields. Therefore, we are going to work in the following with covariant derivatives of the form

$$D_\mu = \partial_\mu - iQ_\Phi^T G A_\mu, \quad (9)$$

where Q_Φ^T is a vector containing the charges of the field Φ with respect to the two Abelian gauge groups and G is the gauge coupling matrix

$$G = \begin{pmatrix} g_R & g_{RBL} \\ g_{BLR} & g_{BL} \end{pmatrix}. \quad (10)$$

A_μ contains the gauge bosons $A_\mu = (A_\mu^R, A_\mu^{BL})^T$. Since the off-diagonal elements in eq. (8) are negative and roughly one order smaller than the diagonal ones, it can be expected that the off-diagonal gauge couplings at the SUSY scale are positive but also much smaller than the diagonal ones. This is in some contrast to models in which kinetic mixing arises due to the presence of $U(1)_Y \times U(1)_{B-L}$ [65]. In addition, a mixing term of the form

$$M_{BLR} \lambda_{BL} \lambda_R \quad (11)$$

between the two gaugino λ_{BL} and λ_R will be present [66]. Since we have chosen the $SU(2)_R$ breaking scale to be very close to the GUT scale we demand as additional boundary conditions that the new parameters arising from kinetic mixing vanish at the GUT scale, *i.e.*

$$g_{RBL} = g_{BLR} = 0, \quad M_{BLR} = 0. \quad (12)$$

For more details on $U(1)$ mixing and its physical impact we refer the interested reader also to recent papers [65, 67–69]. Our focus will be on the additional terms in the scalar mass matrices due to the presence of non-diagonal couplings.

B. Tadpole equations and boundary conditions

The $U(1)_R \times U(1)_{B-L}$ gauge symmetry is spontaneously broken to the hypercharge $U(1)_Y$ by the vevs v_{χ_R} and $v_{\bar{\chi}_R}$ of the scalar components of the $\hat{\chi}_R$ and $\hat{\bar{\chi}}_R$ superfields while the $SU(2)_L \otimes U(1)_Y \rightarrow U(1)_Q$ is governed by the vevs v_d and v_u of the neutral scalar components of the $SU(2)_L$ Higgs doublets H_d and H_u up to gauge kinetic mixing effects. One can write

$$\chi_R = \frac{1}{\sqrt{2}} (\sigma_R + i\varphi_R + v_{\chi_R}), \quad \bar{\chi}_R = \frac{1}{\sqrt{2}} (\bar{\sigma}_R + i\bar{\varphi}_R + v_{\bar{\chi}_R}), \quad (13)$$

$$H_d^0 = \frac{1}{\sqrt{2}} (\sigma_d + i\varphi_d + v_d), \quad H_u^0 = \frac{1}{\sqrt{2}} (\sigma_u + i\varphi_u + v_u), \quad (14)$$

where the generic symbols σ and φ denote the CP-even and CP-odd components of the relevant fields, respectively.

The minimum conditions for the four different vevs can be written at tree-level as

$$t_d = -B_\mu v_u + v_d \left(m_{H_d}^2 + |\mu|^2 + \frac{1}{8} A_{LR,3} (v_d^2 - v_u^2) + \frac{1}{8} A_{LR,2} (v_{\bar{\chi}_R}^2 - v_{\chi_R}^2) \right) \quad (15)$$

$$t_u = -B_\mu v_d + v_u \left(m_{H_u}^2 + |\mu|^2 - \frac{1}{8} A_{LR,3} (v_d^2 - v_u^2) - \frac{1}{8} A_{LR,2} (v_{\bar{\chi}_R}^2 - v_{\chi_R}^2) \right) \quad (16)$$

$$t_{\bar{\chi}_R} = -B_{\mu_R} v_{\chi_R} + v_{\bar{\chi}_R} \left(m_{\bar{\chi}_R}^2 + |\mu_R|^2 + \frac{1}{8} A_{LR,1} (v_{\bar{\chi}_R}^2 - v_{\chi_R}^2) + \frac{1}{8} A_{LR,2} (v_d^2 - v_u^2) \right) \quad (17)$$

$$t_{\chi_R} = -B_{\mu_R} v_{\bar{\chi}_R} + v_{\chi_R} \left(m_{\chi_R}^2 + |\mu_R|^2 - \frac{1}{8} A_{LR,1} (v_{\bar{\chi}_R}^2 - v_{\chi_R}^2) - \frac{1}{8} A_{LR,2} (v_d^2 - v_u^2) \right) \quad (18)$$

where we defined

$$\begin{aligned} A_{LR,1} &= g_{BL}^2 + g_R^2 + g_{BLR}^2 + g_{RBL}^2 - 2g_R g_{BLR} - 2g_{BL} g_{RBL} \\ A_{LR,2} &= g_R^2 + g_{RBL}^2 - g_R g_{BLR} - g_{BL} g_{RBL} \\ A_{LR,3} &= g_L^2 + g_R^2 + g_{RBL}^2. \end{aligned} \quad (19)$$

For the vacuum expectation values we use the following parameterization:

$$\begin{aligned} v_R^2 &= v_{\chi_R}^2 + v_{\bar{\chi}_R}^2, \quad v^2 = v_d^2 + v_u^2 \\ \tan \beta_R &= \frac{v_{\chi_R}}{v_{\bar{\chi}_R}}, \quad \tan \beta = \frac{v_u}{v_d}. \end{aligned} \quad (20)$$

The tadpole equations can analytically be solved for either (i) $(\mu, B_\mu, \mu_R, B_{\mu_R})$ or (ii) $(\mu, B_\mu, m_{\chi_R}^2, m_{\bar{\chi}_R}^2)$ or (iii) $(m_{H_d}^2, m_{H_u}^2, m_{\chi_R}^2, m_{\bar{\chi}_R}^2)$. Option (i) can be considered the minimal version. We call this option CmBLR (constrained mBLR), since it allows to define boundary conditions for all scalar soft masses, $m_{H_d}^2 = m_{H_u}^2 = m_0^2$ and $m_{\chi_R}^2 = m_{\bar{\chi}_R}^2 = m_0^2$ at m_{GUT} , reducing the number of free parameters by four. This assumption, however, leads to some important constraints on the parameter space, as we will discuss next. Options (ii) and (iii) are more flexible. Option (ii) is similar to the CMSSM with non-universal soft masses (NUHM) [70–72], albeit the non-universality is only in the $B - L$ sector. We will call this the χ_R mBLR (non-universal χ_R masses mBLR), and most of our numerical results are based on this option. We mention option (iii) for completeness, but we have not used it in our numerical studies.

As will be shown in section III A, the mass of the Z' -boson in the mBLR model is approximately given by

$$m_{Z'}^2 \simeq \frac{1}{4} A_{LR,1} v_R^2 \quad (21)$$

We can use this expression and eqs (15)-(18) to obtain an approximate relation between $m_{Z'}$ and $\mu_R, m_{\chi_R}^2, m_{\bar{\chi}_R}^2$ and $\tan \beta_R$. This leads to

$$m_{Z'}^2 \simeq -2(|\mu_R|^2 + m_{\bar{\chi}_R}^2) + \frac{g_R^2}{4} v^2 \cos(2\beta) \frac{\tan \beta_R^2 + 1}{\tan \beta_R^2 - 1} + \Delta m_{\chi_R}^2 \frac{2 \tan \beta_R^2}{\tan \beta_R^2 - 1} \quad (22)$$

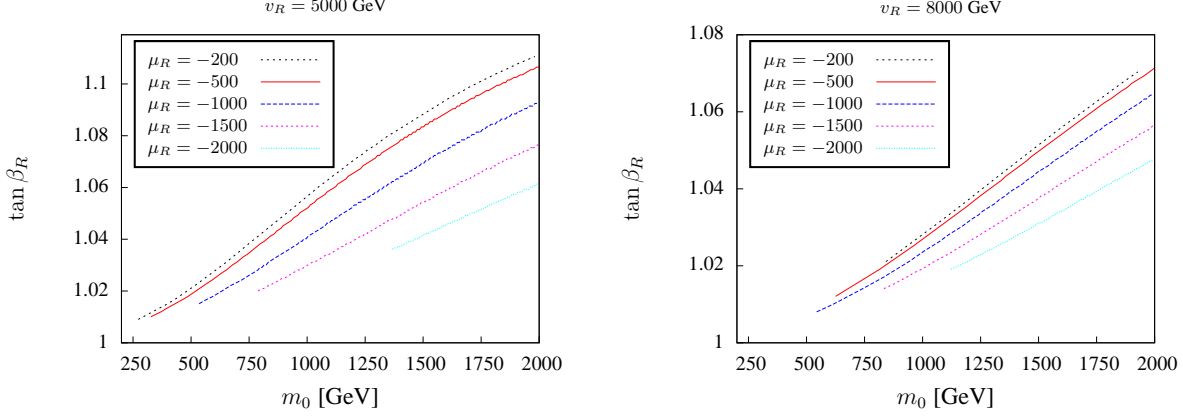


FIG. 1: Constraints on the CmBLR parameter space from the condition of correct symmetry breaking, to the left: $v_R = 5$ TeV, to the right $v_R = 8$ TeV. In both plots $M_{1/2} = 1000$ GeV, $\tan\beta = 10$ and $A_0 = 0$. Just above the lines for $\mu_R = -200$ GeV $|\mu_R|^2 = 0$, i.e. larger values of $\tan\beta_R$ do not lead to consistent solutions of the tadpole equations (for fixed m_0 and A_0). For detailed explanation see text.

where $\Delta m_{\chi_R}^2 = m_{\tilde{\chi}_R}^2 - m_{\chi_R}^2$. We can roughly estimate $\Delta m_{\chi_R}^2$, if we make a mSugra-like assumption for the boundary conditions, $m_{\tilde{\chi}_R}^2 = m_{\chi_R}^2 = m_0^2$ at the GUT scale. The running value of $\Delta m_{\chi_R}^2$ can then be found by a one-step integration of the RGEs at 1-loop level as:

$$\Delta m_{\chi_R}^2 \simeq \frac{1}{4\pi^2} \text{Tr}(Y_s Y_s^\dagger) (3m_0^2 + A_0^2) \log\left(\frac{m_{GUT}}{M_{SUSY}}\right) \quad (23)$$

with $T_s \simeq A_0 Y_s$. As eq.(23) shows, with these assumptions $\Delta m_{\chi_R}^2 > 0$ and the condition that $m_{Z'}$ of eq.(22) has to fulfill the experimental lower bound will define an excluded area in the 3-dimensional parameter space $[\text{Tr}(Y_s Y_s^\dagger), \tan\beta_R, m_{RGE}^2]$, where $m_{RGE}^2 = (3m_0^2 + A_0^2)$. If we assume in addition that Y_s is small enough to remain perturbative anywhere between the weak and the GUT scale, a lower bound on m_{RGE}^2 as a function of $\tan\beta_R - 1$ will result in the CmBLR.

This can be understood in more details as follows. In the CmBLR $\Delta m_{\chi_R}^2 \geq 0$, as shown by eq. (23) and the last term in eq. (22) is positive only if $\tan\beta_R > 1$. Since $\cos(2\beta) < 0$ the second term in eq. (22) is positive only if $\tan\beta_R < 1$. If $\Delta m_{\chi_R}^2 \gtrsim |\frac{g_R^2}{4} v^2 \cos(2\beta)|$, only solutions with $\tan\beta_R > 1$ can be found. Since finally $|\mu_R|^2$ must be $|\mu_R|^2 > 0$ and $m_{\tilde{\chi}_R}^2 > 0$ in the CmBLR we get the constraints on the parameter space shown in fig. 1. Here we show for two choices of v_R contour lines of μ_R in the plane $(\tan\beta_R, m_0)$. Just above the lines for $\mu_R = -200$ GeV $|\mu_R|^2 = 0$, i.e. larger values of $\tan\beta_R$ do not lead to consistent solutions of the tadpole equations (for fixed m_0 and A_0). This restricts the model to values of $\tan\beta_R$ very close to 1, as is clearly demonstrated in the figure. Note that for low values of m_0 the constraints on the viable region of $\tan\beta_R$ actually becomes stronger. ⁶

⁶ $\tan\beta_R \simeq 1$ is also needed for a spectrum without tachyons since the additional D-terms can give large

No such constraint on m_0 and A_0 exists in the χ_R mBLR, since here $\Delta m_{\chi_R}^2$ is a free parameter. However, if $(\Delta m_{\chi_R}^2/m_{\chi_R}^2) \ll 1$, values of $\tan \beta_R$ very close to 1 are preferred by eq. (22) in both, the CmBLR and the χ_R mBLR.

III. MASSES

In this section we give the most important mass matrices of the model at tree-level. In the numerical calculations we take also the 1-loop corrections [73] into account, see appendix for more details. The numerical implementation of the model has been done using **SPheno** [74, 75], for which the necessary subroutines and input files were generated using the package **SARAH** [76–78]. The used model files are included in the public version 3.1.0 of **SARAH**.

A. Gauge bosons

In the basis (W^0, B_{B-L}, B_R) the mass matrix for the neutral gauge bosons reads at tree-level

$$M_{VV}^2 = \frac{1}{4} \begin{pmatrix} g_L^2 v^2 & -g_L g_{RBL} v^2 & -g_L g_R v^2 \\ -g_L g_{RBL} v^2 & g_{RBL}^2 v^2 + \tilde{g}_{BL}^2 v_R^2 & g_R g_{RBL} v^2 - \tilde{g}_R \tilde{g}_{BL} v_R^2 \\ -g_L g_R v^2 & g_R g_{RBL} v^2 - \tilde{g}_R \tilde{g}_{BL} v_R^2 & g_R^2 v^2 + \tilde{g}_R^2 v_R^2 \end{pmatrix} \quad (24)$$

where

$$\tilde{g}_{BL} = (g_{BL} - g_{RBL}), \quad \tilde{g}_R = (g_R - g_{BLR}). \quad (25)$$

From eq. (24) the masses of the photon, the Z and the Z' can be calculated analytically

$$m_\gamma = 0, \quad m_{Z,Z'}^2 = \frac{1}{8} \left(Av^2 + Bv_R^2 \mp v_R^2 \sqrt{-4C \left(\frac{v^2}{v_R^2} \right) + \left(A \left(\frac{v^2}{v_R^2} \right) + B \right)^2} \right) \quad (26)$$

with

$$\begin{aligned} A &= g_L^2 + g_R^2 + g_{RBL}^2 \\ B &= g_{BL}^2 + g_R^2 + g_{BLR}^2 + g_{RBL}^2 - 2g_{BLR}g_R - 2g_{RBL}g_{BL} \\ C &= g_L^2(g_R - g_{BLR})^2 + g_{BL}^2(g_L^2 + g_R^2) - 2g_{BL}(g_L^2 + g_{BLR}g_R)g_{RBL} + (g_{BLR}^2 + g_L^2)g_{RBL}^2. \end{aligned} \quad (27)$$

Expanding eq. 26 in powers of v^2/v_R^2 , we find up to first order

$$m_Z^2 = \frac{Cv^2}{4B}, \quad m_{Z'}^2 = \frac{(AB - C)v^2 + B^2v_R^2}{4B}. \quad (28)$$

In the limit $g_{BLR} = 0$ and $g_{RBL} = 0$ we then get

$$m_Z^2 = \frac{(g_{BL}^2 g_L^2 + g_{BL}^2 g_R^2 + g_L^2 g_R^2)v^2}{4(g_{BL}^2 + g_R^2)}, \quad m_{Z'}^2 = \frac{g_R^4 v^2}{4(g_{BL}^2 + g_R^2)} + \frac{1}{4}(g_{BL}^2 + g_R^2)v_R^2. \quad (29)$$

negative contributions to the sfermion masses, see below.

ATLAS has recently published updated lower limits on Z' searches [79]. Our Z' corresponds to the Z_χ in the notation of [80], i.e. [79] gives a lower limit of $Z' \gtrsim 1.8$ TeV, which corresponds to roughly $v_R \gtrsim 5$ TeV for our choice of couplings⁷, see, however, the discussion in section IV C.

Mixing between Z and Z' states lead to a shift in the ρ -parameter [81], measured very accurately at LEP [82]. Expanding eq. 26 up to second order, we estimate the shift to be of order

$$\Delta\rho = \frac{v^2/v_R^2}{v^2/v_R^2 + B^2/(C - 2AB)} . \quad (30)$$

For our choice of couplings g_L , g_R and g_{B-L} (fixed by the experimental inputs and gauge coupling unification) this leads to a lower limit of roughly $v_R \gtrsim 3.3$ TeV, similar to but less stringent than the direct search bound.

B. Higgs bosons

1. Pseudoscalar Higgs bosons

At the tree level we find that in the $(\varphi_d, \varphi_u, \bar{\varphi}_R, \varphi_R)$ basis the pseudoscalar sector has a block-diagonal form and reads in Landau gauge

$$M_{AA}^2 = \begin{pmatrix} M_{AA,L}^2 & 0 \\ 0 & M_{AA,R}^2 \end{pmatrix} \quad (31)$$

with

$$M_{AA,L}^2 = B_\mu \begin{pmatrix} \tan\beta & 1 \\ 1 & \cot\beta \end{pmatrix}, \quad M_{AA,R}^2 = B_{\mu_R} \begin{pmatrix} \tan\beta_R & 1 \\ 1 & \cot\beta_R \end{pmatrix}. \quad (32)$$

From these four states two are Goldstone bosons which become the longitudinal parts of the massive neutral vector bosons Z and a Z' . In the physical spectrum there are two pseudoscalars A^0 and A_R^0 with masses

$$m_A^2 = B_\mu(\tan\beta + 1/\tan\beta), \quad m_{A_R}^2 = B_{\mu_R}(\tan\beta_R + 1/\tan\beta_R). \quad (33)$$

⁷ The condition that the gauge couplings reproduce correctly the standard model hypercharge, plus the assumption of unification lead to values of roughly $g_{BL} \sim 0.57$, $g_R \sim 0.45$, $g_{BLR} \sim 0.014$ and $g_{RBL} \sim 0.012$ at the SUSY scale.

2. Scalar Higgs bosons

The tree-level CP-even Higgs mass matrix in the $(\sigma_d, \sigma_u, \bar{\sigma}_R, \sigma_R)$ basis reads

$$M_{hh}^2 = \begin{pmatrix} m_{LL}^2 & m_{LR}^2 \\ m_{LR}^{2,T} & m_{RR}^2 \end{pmatrix}, \quad (34)$$

where

$$m_{LL}^2 = \begin{pmatrix} (g_Z^2 + \frac{1}{4}g_{RBL}^2)v^2c_\beta^2 + m_A^2s_\beta^2 & -\frac{1}{2}(m_A^2 + (g_Z^2 + \frac{1}{4}g_{RBL}^2)v^2)s_{2\beta} \\ -\frac{1}{2}(m_A^2 + (g_Z^2 + \frac{1}{4}g_{RBL}^2)v^2)s_{2\beta} & (g_Z^2 + \frac{1}{4}g_{RBL}^2)v^2s_\beta^2 + m_A^2c_\beta^2 \end{pmatrix}, \quad (35)$$

$$m_{LR}^2 = \frac{1}{4} \begin{pmatrix} (\tilde{g}_R g_R - \tilde{g}_{BL} g_{RBL}) v v_R c_\beta c_{\beta_R} & -(\tilde{g}_R g_R - \tilde{g}_{BL} g_{RBL}) v v_R c_\beta s_{\beta_R} \\ -(\tilde{g}_R g_R - \tilde{g}_{BL} g_{RBL}) v v_R s_\beta c_{\beta_R} & (\tilde{g}_R g_R - \tilde{g}_{BL} g_{RBL}) v v_R s_\beta s_{\beta_R} \end{pmatrix}, \quad (36)$$

$$m_{RR}^2 = \begin{pmatrix} \tilde{g}_{Z_R}^2 v_R^2 c_{\beta_R}^2 + m_{A_R}^2 s_{\beta_R}^2 & -\frac{1}{2}(m_{A_R}^2 + \tilde{g}_{Z_R}^2 v_R^2) s_{2\beta_R} \\ -\frac{1}{2}(m_{A_R}^2 + \tilde{g}_{Z_R}^2 v_R^2) s_{2\beta_R} & \tilde{g}_{Z_R}^2 v_R^2 s_{\beta_R}^2 + m_{A_R}^2 c_{\beta_R}^2 \end{pmatrix}, \quad (37)$$

$s_x = \sin(x)$, $c_x = \cos(x)$ ($x = \beta, \beta_R, 2\beta, 2\beta_R$), $g_Z^2 = (g_L^2 + g_R^2)/4$, $\tilde{g}_{Z_R}^2 = (\tilde{g}_{BL}^2 + \tilde{g}_R^2)/4$. The matrix m_{LL}^2 contains the standard MSSM doublet mass matrix. To see this explicitly one has to integrate out the additional Higgs fields in the $v_R \rightarrow \infty$ limit which yields a shift in the gauge couplings such that the MSSM limit is achieved. m_{RR}^2 corresponds to the $U(1)_R \times U(1)_{B-L}$ Higgs bosons and m_{LR}^2 provides the essential mixing between the two sectors.

Note that it is straightforward to show that the determinant of the mass matrix eq. (34) goes to zero, whenever one of the parameters $((\tan \beta - 1), m_A, (\tan \beta_R - 1), m_{A_R})$ goes to zero. One can also calculate analytically that in the limit of $v_R \rightarrow \infty$ the lightest eigenvalue of eq. (34) obeys the MSSM tree-level limit for h^0 . For finite v_R corrections to m_{LL}^2 appear, of the order of $g_R^2 v^3 / v_R$, which lead to a shift in the lightest eigenvalue. Thus the MSSM tree-level upper bound of $m_{h^0}^{\text{tree}} \leq m_{Z^0}$ for the lightest Higgs can be violated.

3. Numerical examples

In fig. 2 we show the two lightest Higgs boson masses (to the left) together with

$$\mathcal{R}_{Li}^2 \equiv R_{i1}^2 + R_{i2}^2 \quad (38)$$

(to the right) as a function of v_R . Here $i = 1, 2$ labels the light Higgs scalars in the model and R_{ij} is the rotation matrix which diagonalizes the CP-even Higgs sector. Note that the quantity \mathcal{R}_{Li}^2 , which reaches one in the MSSM limit, is a rough measure of how much the corresponding Higgs with index i resembles an MSSM Higgs boson. We will call this leftness. Roughly speaking, the smaller this quantities is, the smaller is the i -th Higgs coupling to the Z - and W -bosons, implying a reduced production cross sections at LEP, Tevatron and the LHC.

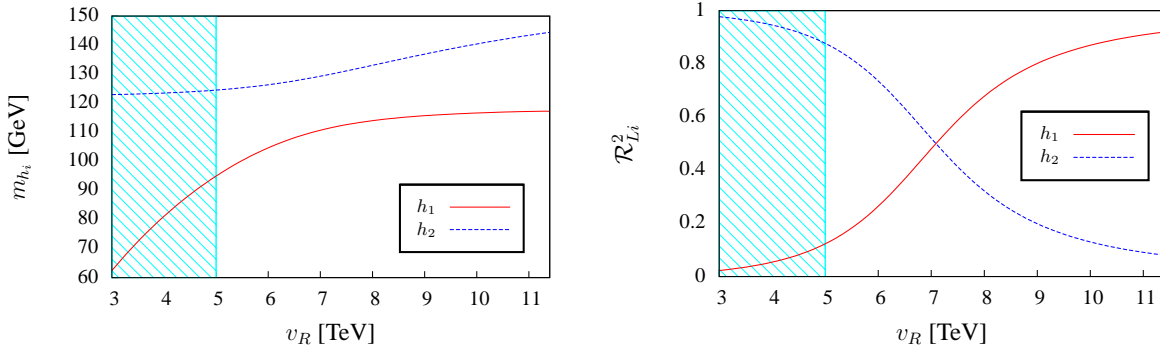


FIG. 2: Example plot for the masses (left) and “leftness” (right) of two lightest eigenvalues of the CP-even Higgs sector as a function of v_R for fixed choices of the other parameters: $m_0 = 250$ GeV, $M_{1/2} = 800$ GeV, $\tan \beta = 10$, $A_0 = 0$, $\tan \beta_R = 0.94$, $\mu_R = -800$ GeV, $m_{A_R} = 2350$ GeV.

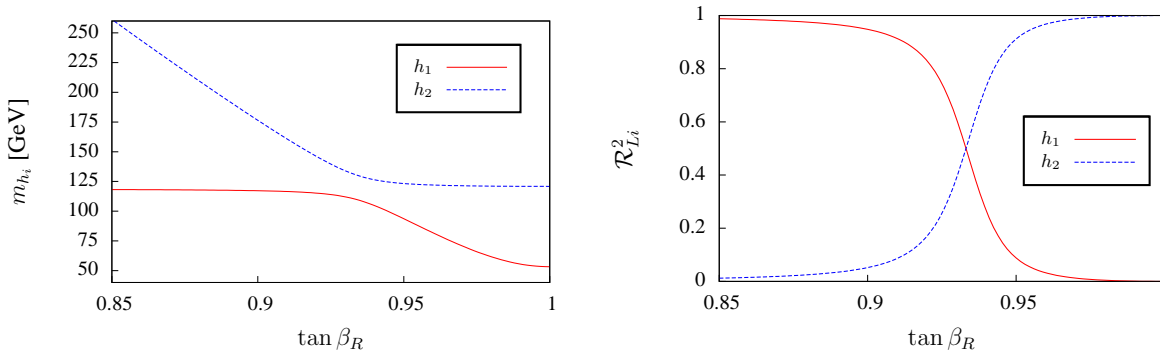


FIG. 3: Example plot for the masses (left) and “leftness” (right) of two lightest eigenvalues of the CP-even Higgs sector as a function of $\tan \beta_R$ for fixed choices of the other parameters: $m_0 = 250$ GeV, $M_{1/2} = 800$ GeV, $\tan \beta = 10$, $A_0 = 0$, $v_R = 6000$ GeV, $\mu_R = -800$ GeV, $m_{A_R} = 2350$ GeV

Since the MSSM Higgs and the two additional Higgs χ_R and $\bar{\chi}_R$ are both charged under $U(1)_R$ the two lightest Higgs states mix due to additional D-terms in the CP-even Higgs matrix (see eq. (35)). Thus, both the masses and the mixing of the two lightest Higgs h_1 and h_2 depend strongly on v_R , see fig. 2. In this example, up to approximately $v_R=6$ TeV h_1 is mostly the singlet Higgs whereas h_2 is the MSSM-like Higgs. For larger v_R a level-crossing occurs and the situation is reversed. Note that, although m_0 , $M_{1/2}$ and A_0 have rather moderate values in this example, h_2 has a mass of the order of $m_{h_2} \simeq 125$ GeV for $v_R \simeq 5 - 6$ TeV, i.e. the D-terms have shifted the MSSM-like Higgs mass into the region preferred by ATLAS and CMS.

In fig. 3 masses and “leftness” of the two lightest Higgs eigenstates are plotted against $\tan \beta_R$. For $\tan \beta_R$ close to $\tan \beta_R = 1$ one gets a very light singlet Higgs as expected, see discussion above. As is the case when varying v_R a level-crossing appears also when $\tan \beta_R$

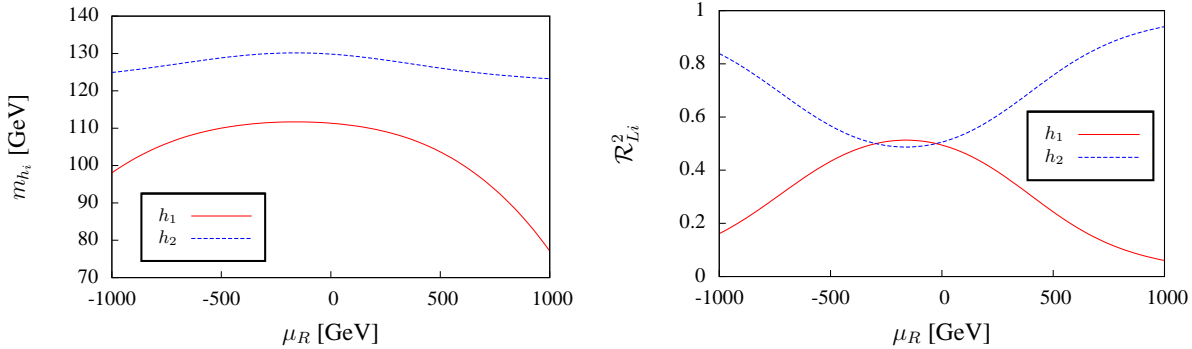


FIG. 4: Example plot for the masses (left) and “leftness” (right) of two lightest eigenvalues of the CP-even Higgs sector as a function of μ_R for fixed choices of the other parameters: $m_0 = 250$ GeV, $M_{1/2} = 800$ GeV, $\tan \beta = 10$, $A_0 = 0$, $v_R = 6000$ GeV, $\tan \beta_R = 0.94$, $m_{A_R} = 2350$ GeV

is changed. In this figure the χ_R mBLR version was used, thus we can put $\tan \beta_R < 1$. Note, however, that the masses of h_1 and h_2 show a behavior which is symmetric with respect to $|\tan \beta_R - 1|$. Again the figure demonstrates that the MSSM limit of the lightest Higgs mass can be violated at the expense of a reduced coupling of the MSSM-like state to SM gauge bosons.

1-loop corrections play in general an important role, not only for the MSSM-like Higgs but also in the singlet sector. This can be seen in fig. 4, where we plot masses and mixings of h_1 and h_2 versus the parameter μ_R . Increasing or decreasing μ_R , respectively, changes the mass of the mostly-singlet Higgs by considerable factors. In fact, for larger values of $|\mu_R|$ one can get easily a negative mass squared for h_1 , which is of course forbidden phenomenologically. The importance of μ_R stems from 1-loop contributions to the Higgs mass matrix with a higgsino-right in the loop. Loop corrections for the mostly-singlet Higgs are, in fact, even more important numerically than for the MSSM-like Higgs and many points which are allowed at tree-level lead to tachyonic states, once 1-loop corrections are taken into account.

Finally we note, that in the plots in this section we have not shown the regions excluded by LEP or the LHC searches, since we were interested only in showing the parameter dependencies of our numerical results. In the study points of the next section, however, we have taken care that our points survive all known experimental constraints.

C. Neutrinos

The mBLR model contains beside the usual three left-handed neutrinos six additional states which are singlets with respect to the SM group. The corresponding mass matrix is

in the basis (ν_L, ν^c, S) given by

$$m_\nu = \begin{pmatrix} 0 & \frac{1}{\sqrt{2}}v_u Y_\nu^T & 0 \\ \frac{1}{\sqrt{2}}v_u Y_\nu & 0 & \frac{1}{\sqrt{2}}v_{\chi_R} Y_s \\ 0 & \frac{1}{\sqrt{2}}v_{\chi_R} Y_s^T & \mu_S \end{pmatrix}. \quad (39)$$

This matrix is diagonalized by U^ν :

$$U^{\nu,*} m_\nu U^{\nu,\dagger} = m_\nu^{dia}. \quad (40)$$

Eigenvalues for the three light (and mostly left-handed) neutrinos can be found in the seesaw approximation as:

$$m_\nu^{\text{eff}} = -\frac{v_u^2}{v_R^2} Y_\nu^T (Y_s^T)^{-1} \mu_S Y_s^{-1} Y_\nu. \quad (41)$$

Neutrino data implies that either Y_ν and/or μ_S is small and in inverse seesaw the smallness of neutrino mass is attributed to the smallness of the latter. As we will discuss in section IV A, the bounds on rare lepton decays imply that the off-diagonal terms of Y_s and Y_ν have to be small compared to their diagonal entries, unless their diagonal values are small too.

The smallness of μ_S implies that the six heavy states form three ‘‘quasi-Dirac’’ pairs. For vanishing off-diagonal entries in Y_s and Y_ν a good estimate of the masses of the heavy states is:

$$m_{\nu_h,ii} \simeq \pm \sqrt{|Y_{\nu,ii}|^2 v_u^2 + |Y_{s,ii}|^2 v_{\chi_R}^2}. \quad (42)$$

D. Sparticles

1. Neutralinos

The mass matrix of the neutralinos reads in the basis $(\lambda_{BL}, \lambda_L^0, \tilde{h}_d^0, \tilde{h}_u^0, \lambda_R, \tilde{\chi}_R, \tilde{\chi}_R)$:

$$M_{\tilde{\chi}^0} = \begin{pmatrix} M_{BL} & 0 & -\frac{1}{2}g_{RBL}v_d & \frac{1}{2}g_{RBL}v_u & \frac{M_{BLR}}{2} & \frac{1}{2}v_{\tilde{\chi}_R}\tilde{g}_{BL} & -\frac{1}{2}v_{\tilde{\chi}_R}\tilde{g}_{BL} \\ 0 & M_2 & \frac{1}{2}g_L v_d & -\frac{1}{2}g_L v_u & 0 & 0 & 0 \\ -\frac{1}{2}g_{RBL}v_d & \frac{1}{2}g_L v_d & 0 & -\mu & -\frac{1}{2}g_R v_d & 0 & 0 \\ \frac{1}{2}g_{RBL}v_u & -\frac{1}{2}g_L v_u & -\mu & 0 & \frac{1}{2}g_R v_u & 0 & 0 \\ \frac{M_{BLR}}{2} & 0 & -\frac{1}{2}g_R v_d & \frac{1}{2}g_R v_u & M_R & -\frac{1}{2}v_{\tilde{\chi}_R}\tilde{g}_R & \frac{1}{2}v_{\tilde{\chi}_R}\tilde{g}_R \\ \frac{1}{2}v_{\tilde{\chi}_R}\tilde{g}_{BL} & 0 & 0 & 0 & -\frac{1}{2}v_{\tilde{\chi}_R}\tilde{g}_R & 0 & -\mu_R \\ -\frac{1}{2}v_{\tilde{\chi}_R}\tilde{g}_{BL} & 0 & 0 & 0 & \frac{1}{2}v_{\tilde{\chi}_R}\tilde{g}_R & -\mu_R & 0 \end{pmatrix}. \quad (43)$$

The eigenvalues of this matrix are not completely arbitrary. Since $U(1)_{B-L} \times U(1)_R$ is broken in such a way as to produce correctly the SM group $U(1)_Y$ in the limit of $v \ll v_R$ the matrix contains one state which corresponds to the MSSM bino, \tilde{B} , which is a superposition of λ_{BL} and λ_R . In addition the matrix contains an orthogonal state, which we will call \tilde{B}_\perp in the following.

For CMSSM like boundary conditions, $M_{BL} = M_2 = M_R = M_{1/2}$, the bino is usually the lightest of the three gaugino like states, with the \tilde{W} being approximately twice as heavy. The \tilde{B}_\perp is very often mixed with one of the right higgsinos, and, since M_{BL} at low energies is much smaller than v_R this mixing is often important. In addition, there is the standard quasi-Dirac pair of “left” higgsinos, plus two more states which are mostly right higgsinos. Of the latter one is usually rather heavy, while the other can be light, if μ_R is small.

In fig. 5 the neutralino masses and $\mathcal{R}_{\perp i}^2$ for CmBLR are plotted against v_R for some arbitrary choice of other parameters. As discussed, there are in total seven eigenstates. Of special interest is the \tilde{B}_\perp , so in the plot on the right we show the percentage of \tilde{B}_\perp ($\mathcal{R}_{\perp i}^2$) in the corresponding mass eigenstate. Here $\mathcal{R}_{\perp i}^2 = 1$ means that the i -th neutralino is a pure \tilde{B}_\perp . As one can see in fig. 6 the masses and mixing of the three new states depend strongly on v_R . For small v_R all three states mix to each other. Increasing v_R leads to a decoupling of the lighter higgsino-right from the \tilde{B}_\perp which decreases in mass since μ_R becomes smaller for large v_R while the masses of the two remaining states get large. Since the MSSM Neutralinos mix very little with the new states, there are four eigenvalues which show almost no dependence on the parameters v_R and μ_R .

In fig. 6 the neutralino masses and $\mathcal{R}_{\perp i}^2$ are plotted against v_R for the case of χ_R mBLR. In this calculation, μ_R and m_{A_R} can take fixed values while v_R is varied freely. Two of the three new Neutralino states are a mixture of the higgsino-right and \tilde{B}_\perp and therefore depend on v_R . Since the lighter higgsino-right hardly mix to the \tilde{B}_\perp it has a constant mass at $m_{\tilde{h}_R} \simeq |\mu_R| = 1700$ GeV in this example. The lighter of the two new states that show dependence on v_R is mostly a \tilde{B}_\perp , whereas the one with larger mass is mostly a higgsino-right. The smaller v_R the smaller the mixing between these two states and thus the larger the coupling of the mostly \tilde{B}_\perp -state to the MSSM particles. This will be important when we discuss LHC phenomenology in section IV E.

The dependence of the neutralino masses and $\mathcal{R}_{\perp i}^2$ on μ_R is shown in fig. 7. Since the higgsino-right and the \tilde{B}_\perp mix, all three states show a dependence on μ_R . The state which hardly mixes to the \tilde{B}_\perp decreases in mass for small $|\mu_R|$. So we can easily have a higgsino-right as LSP choosing μ_R close to zero. The state which is mostly the \tilde{B}_\perp gets a smaller mass for large $|\mu_R|$, while the one which is mostly a higgsino-right increases in mass.

2. Sleptons and sneutrinos

In models in which lepton number is broken, the scalar neutrinos split into a real and an imaginary part with slightly different masses [83]. Since we assume that the smallness of neutrino masses is due to the smallness of the parameter μ_S (and, therefore, B_{μ_S} is supposed to be small too), this splitting between sneutrino mass eigenstates is too small to be of any relevance, except neutrino masses themselves.

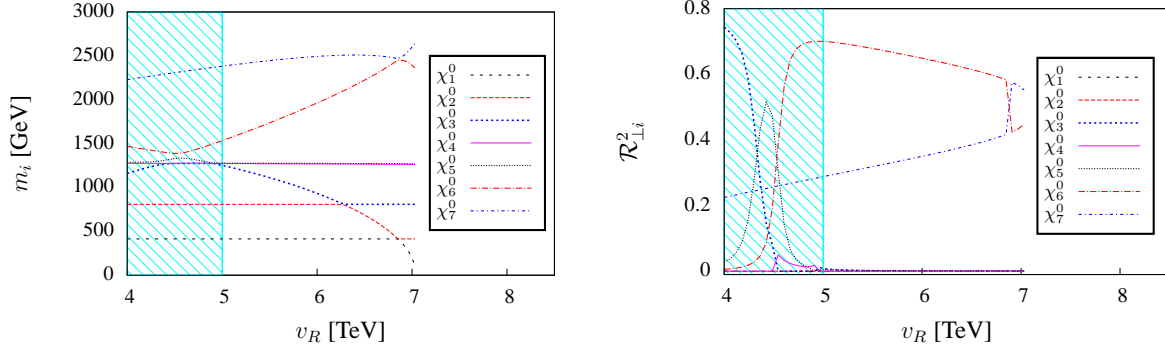


FIG. 5: Neutralino masses (left) and $\mathcal{R}_{\perp i}^2$ (right) versus v_R for otherwise fixed choice of parameters: $m_0 = 1000$ GeV, $M_{1/2} = 1000$ GeV, $\tan\beta = 10$, $A_0 = -600$, $\tan\beta_R = 1.04$. This plot uses the CmBLR version of the model.

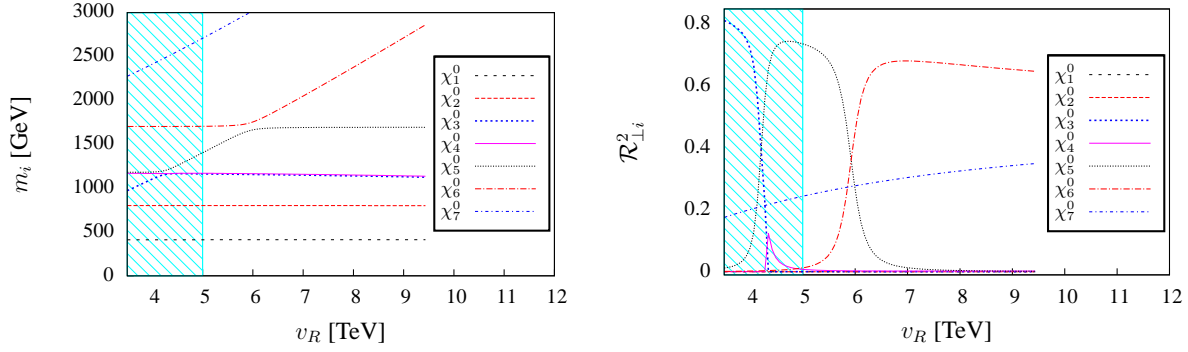


FIG. 6: Neutralino masses (left) and $\mathcal{R}_{\perp i}^2$ (right) versus v_R for otherwise fixed choice of parameters: $m_0 = 630$ GeV, $M_{1/2} = 1000$ GeV, $\tan\beta = 10$, $A_0 = 0$, $\tan\beta_R = 1.05$, $\mu_R = -1700$ GeV, $m_{A_R} = 4800$ GeV. This plot uses the χ_R mBLR version of the model.

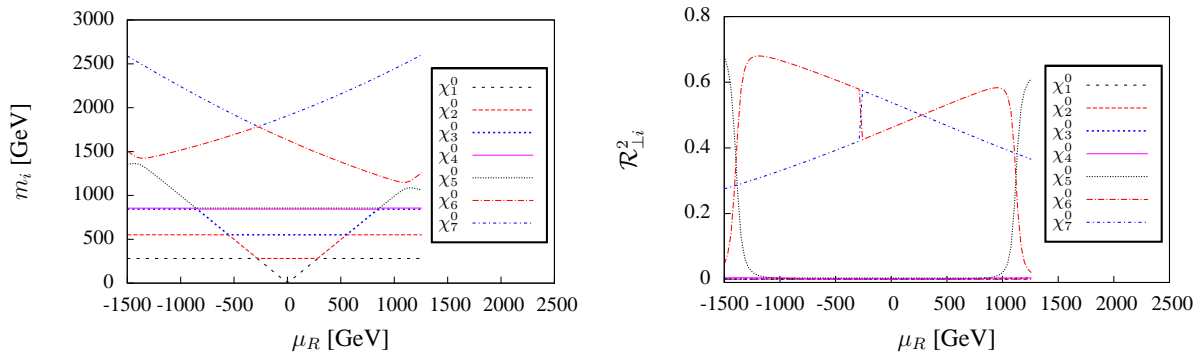


FIG. 7: Neutralino masses (left) and $\mathcal{R}_{\perp i}^2$ (right) versus μ_R for otherwise fixed choice of parameters: $m_0 = 400$ GeV, $M_{1/2} = 700$ GeV, $\tan\beta = 10$, $A_0 = 0$, $v_R = 5000$ GeV, $\tan\beta_R = 1.05$, $m_{A_R} = 3000$ GeV.

Neglecting μ_S and B_{μ_S} the sneutrino mass matrix is given by

$$M_{\tilde{\nu}}^2 = \begin{pmatrix} m_{LL,\tilde{\nu}}^2 & \frac{1}{\sqrt{2}}v_u(T_\nu^\dagger - Y_\nu^\dagger \cot \beta\mu) & \frac{1}{2}v_u v_{\chi_R} Y_\nu^\dagger Y_s \\ \frac{1}{\sqrt{2}}v_u(T_\nu - Y_\nu \cot \beta\mu^*) & m_{RR,\tilde{\nu}}^2 & \frac{1}{\sqrt{2}}v_{\chi_R}(T_s - Y_s \cot \beta_R \mu_R^*) \\ \frac{1}{2}v_u v_{\chi_R} Y_s^\dagger Y_\nu & \frac{1}{\sqrt{2}}v_{\chi_R}(T_s^\dagger - Y_s^\dagger \cot \beta_R \mu_R) & m_S^2 + \frac{v_{\chi_R}^2}{2} Y_s^\dagger Y_s \end{pmatrix} \quad (44)$$

where

$$\begin{aligned} m_{LL,\tilde{\nu}}^2 &= m_L^2 + \frac{v_u^2}{2} Y_\nu^\dagger Y_\nu - \\ &\quad \frac{1}{8} \left((g_{BL}^2 + g_{BLR}^2 - g_{BL}g_{RBL})(v_{\tilde{\chi}_R}^2 - v_{\chi_R}^2) + (g_L^2 + g_R^2 + g_{BL}g_{RBL})(v_d^2 - v_u^2) \right) \mathbf{1} \\ m_{RR,\tilde{\nu}}^2 &= m_\nu^2 + \frac{v_u^2}{2} Y_\nu Y_\nu^\dagger + \frac{v_{\chi_R}^2}{2} Y_s^\dagger Y_s + \\ &\quad \frac{1}{8} \left((g_{BL}^2 + g_R^2 + g_{BLR}^2 + g_{RBL}^2 - 2g_{BL}g_{RBL} - 2g_Rg_{BLR})(v_{\tilde{\chi}_R}^2 - v_{\chi_R}^2) + \right. \\ &\quad \left. (g_R^2 + g_{RBL}^2 - g_{BL}g_{RBL} - g_Rg_{BLR})(v_d^2 - v_u^2) \right) \mathbf{1} \end{aligned} \quad (45)$$

For charged sleptons one gets:

$$M_{\tilde{l}}^2 = \begin{pmatrix} m_{LL,\tilde{l}}^2 & \frac{1}{\sqrt{2}}v_d(T_l^\dagger - Y_l^\dagger \tan \beta\mu) \\ \frac{1}{\sqrt{2}}v_d(T_l - Y_l \tan \beta\mu^*) & m_{RR,\tilde{l}}^2 \end{pmatrix} \quad (46)$$

where

$$\begin{aligned} m_{LL,\tilde{l}}^2 &= m_L^2 + \frac{v_d^2}{2} Y_l^\dagger Y_l - \frac{1}{8} \left((g_{BL}^2 + g_{BLR}^2 - g_{BL}g_{RBL} - g_Rg_{BLR})(v_{\tilde{\chi}_R}^2 - v_{\chi_R}^2) \right. \\ &\quad \left. - (g_L^2 - g_{BL}g_{RBL} - g_Rg_{BLR})(v_d^2 - v_u^2) \right) \mathbf{1} \\ m_{RR,\tilde{l}}^2 &= m_E^2 + \frac{v_d^2}{2} Y_l Y_l^\dagger + \frac{1}{8} \left((g_{BL}^2 - g_R^2 + g_{BLR}^2 - g_{RBL}^2)(v_{\tilde{\chi}_R}^2 - v_{\chi_R}^2) \right. \\ &\quad \left. - (g_R^2 + g_{RBL}^2 + g_{BL}g_{RBL} + g_Rg_{BLR})(v_d^2 - v_u^2) \right) \mathbf{1} \end{aligned} \quad (47)$$

In fig. 8 sneutrino and slepton masses are plotted against v_R , $\tan \beta_R$ and μ_R . The figures on the left show a zoom into the region of the lightest states, whereas the figures on the right show a larger range of masses for a better understanding of the overall behavior. To see which particle is the LSP, while varying v_R , $\tan \beta_R$ and μ_R , we included in all plots on the left the mass of the lightest neutralino state. This state is always a Bino, except for the plot against μ_R . Here the LSP becomes a higgsino-right for $|\mu_R| < 250$ GeV. The plots show that the masses depend strongly on the choice of v_R and $\tan \beta_R$. In the case of charged sleptons the dependence on v_R and $\tan \beta_R$ comes only from additional D-terms at the tree level. This is different for sneutrinos. Here we can have an interplay between new D-terms and terms coming from the coupling Y_s which both depend on v_R and $\tan \beta_R$. The additional D-terms force left sparticle to become light for $\tan \beta_R < 1$ while for $\tan \beta_R > 1$ right sparticle masses

decrease. Up to $v_R = 6$ TeV $\tilde{\nu}_1$ is a right handed sneutrino and therefore the mass increase for increasing v_R . For $v_R > 6$ TeV the mass of $\tilde{\nu}_1$ drops down again since here it is mainly a left handed sneutrino. Thus, increasing v_R leads to a level-crossing in the mass spectrum of left and right handed sneutrinos. The same holds for the sleptons. In the plot against v_R the mass of the right sneutrino decreases much faster for $v_R < 6$ TeV than the mass of the right sleptons. This is due to the off-diagonal terms proportional to Y_s , which contain also μ_R in the sneutrino mass matrix. These terms mix the scalar component of \hat{S} to $\tilde{\nu}_R$. Thus for low values of v_R in this example the LSP is neutral, which is allowed, whereas for larger values of v_R (with left sleptons being light) there are parts of the parameter space, where the lightest slepton is charged, which is phenomenologically forbidden. Whether in the left sector charged or neutral states are lighter, depends heavily on the choice of parameters.

Varying $\tan \beta_R$ the right slepton masses decrease faster than the right sneutrino masses for $\tan \beta_R > 0.95$ due the additional sneutrino mixing. Since the sneutrino and slepton masses depend strongly on the choice of v_R , $\tan \beta_R$ and μ_R one obtains limits on combination on these parameters. On the one hand, one has to avoid tachyonic states and on the other hand one has to take care not to get charged sleptons as LSP. The combination of both conditions forces us to choose $\tan \beta_R$ close to one and gives us an upper limit on v_R and $|\mu_R|$ as function of $|\tan \beta_R - 1|$.

IV. CONSTRAINTS, SAMPLE SPECTRA AND DECAYS

In this section we discuss several interesting phenomenological aspects which potentially allow the BLR model to be discriminated from the MSSM at the LHC and exemplify the most important features for a few study points. We include a discussion of the direct production of new states and characteristic changes in the cascade decays of supersymmetric particles.

For brevity we will call these benchmark points BLRSP1- BLRSP5, the corresponding input parameters are listed in table II. All of these points have been calculated with the χ_R mBLR version of the model. However, note that for BLRSP5 the input is chosen to be consistent with the CmBLR variant.

A few comments on the input parameters and the resulting mass spectra are in order, before we discuss the phenomenology in detail. As shown below, the bounds on rare lepton flavour violating decays require Y_ν and Y_s to be essentially flavour-diagonal, unless these couplings are very small. Therefore we have chosen Y_ν and Y_s diagonal as starting point implying that all points satisfy trivially the LFV constraints. A correct explanation for the neutrino angles then requires flavour violating entries in the parameter μ_S , which we do not give in table II, since they are irrelevant for collider phenomenology.

The input values of table II lead to the mass spectrum shown in tables III and IV. We give the masses and in brackets the particle character. In case of mixed states the two largest components, for example (\tilde{W}, \tilde{h}_L) , are given where the first entry accounts for the larger contribution. If the ordering in the composition changes like in the case of $m_{\tilde{u}_{5,6}}$ we use squared brackets. Therefore we have $(\tilde{c}_L, \tilde{u}_L)$ for $m_{\tilde{u}_5}$ and $(\tilde{u}_L, \tilde{c}_L)$ for $m_{\tilde{u}_6}$. In all cases

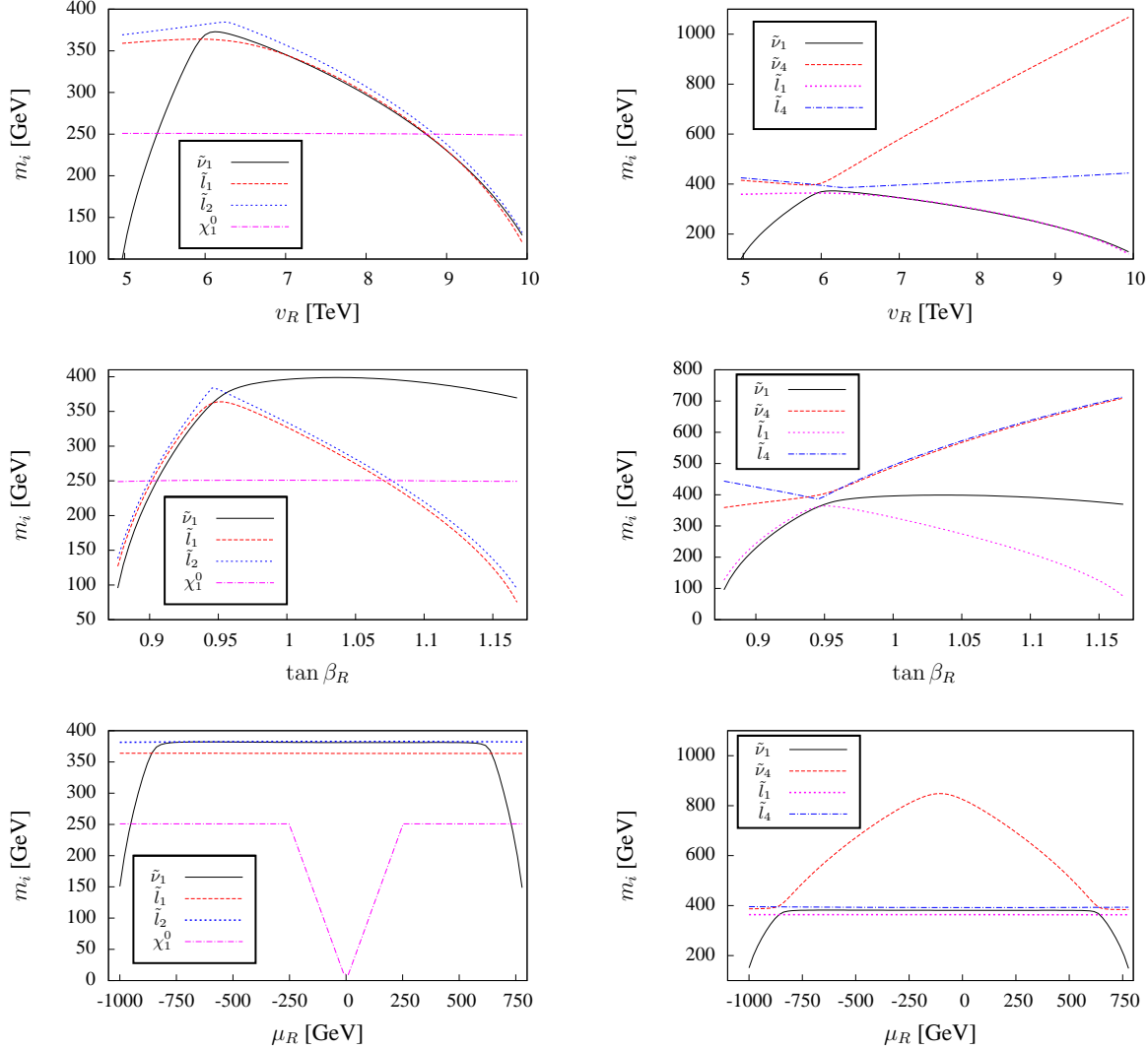


FIG. 8: Lightest slepton (and neutralino) masses as function of v_R , $\tan \beta_R$ and μ_R for a fixed but arbitrary choice of other parameters: $m_0 = 220$ GeV, $M_{1/2} = 630$ GeV, $\tan \beta = 10$, $A_0 = 0$, $\tan \beta_R = 0.95$, $v_R = 6000$, $\mu_R = -850$ GeV, $m_{A_R} = 2200$ GeV, $Y_{s,ii} = 0.3$. Plots on the left show a zoom into the light mass region, such that mass differences between the lightest sneutrino and the lightest charged slepton are resolved, figures to the right show the overall dependence, for a discussion see text.

input parameters have been chosen such, that the squark and gluino masses are outside the region currently excluded by pure CMSSM searches at ATLAS [44] and CMS [45]. Since (a) we expect the missing momentum signal to be smaller in these points than in a true CMSSM spectrum and (b) our squark spectra are less degenerate than the CMSSM case, we believe this is a conservative choice. Two of the points have a sneutrino LSP (BLRSP1 and BLRSP3), while three points have a neutralino LSP (for BLRSP2 and BLRSP5 mostly a bino, for BLRSP4 a state which is mostly a \tilde{h}_R).

	BLRSP1	BLRSP2	BLRSP3	BLRSP4	BLRSP5
cMSSM					
m_0 [GeV]	470	1000	120	165	500
$M_{1/2}$ [GeV]	700	1000	780	700	850
$\tan \beta$	20	10	10	10	10
A_0	0	-3000	-300	0	-600
Extended gauge sector					
v_R [GeV]	4700	6000	6000	5400	5000
$\tan \beta_R$	1.05	1.025	0.85	1.06	1.023
μ_R [GeV]	-1650	-780	-1270	260	(-905)
m_{A_R} [GeV]	4800	7600	800	2350	(1482)
Yukawas					
$Y_{\nu,11}$	0.04	0.1	0.1	0.1	0.1
$Y_{\nu,22}$	0.04	0.1	0.1	0.1	0.1
$Y_{\nu,33}$	0.04	0.1	0.1	0.1	0.1
$Y_{s,11}$	0.04	0.042	0.3	0.3	0.3
$Y_{s,22}$	0.05	0.042	0.3	0.3	0.3
$Y_{s,33}$	0.05	0.042	0.3	0.3	0.3

TABLE II: Parameters of the various study points. In BLRSP1-BLRSP4 μ_R and m_{A_R} are input whereas in BLRSP5 the constrained version of the model has been used and, thus, these two parameters are output. For a discussion of these points see text.

Note that the ordering of sfermion mass eigenstates does in many cases not follow the standard CMSSM patterns: $m_{\tilde{\tau}_1} \leq m_{\tilde{\mu}_R} \simeq m_{\tilde{e}_R} < m_{\tilde{\mu}_L} \simeq m_{\tilde{e}_L} \leq m_{\tilde{\tau}_2}$ and $m_{\tilde{t}_1} \leq m_{\tilde{c}_R} \simeq m_{\tilde{u}_R} < m_{\tilde{c}_L} \simeq m_{\tilde{u}_L} \leq m_{\tilde{t}_2}$ (similar for sdowns). These patterns are distorted in the study points due to the unconventional D-terms of the model and this feature gets enhanced for larger $|\tan \beta_R - 1|$ and/or larger values of v_R . We note also that for sneutrinos and charged sleptons many states are quite degenerate. For example $\tilde{\mu}_R$ and \tilde{e}_R have practically the same mass in all points. While these degeneracies are always true in CMSSM spectra, in our case this is not necessarily so, but simply reflects the fact that both Y_ν and Y_s have been chosen generation independent in all points, except BLRSP1. As this point shows, even a rather moderate generation dependent value of Y_s can lead to large mass splittings in the sneutrino sector. A generation dependent value of Y_ν would not only split sneutrino masses but also charged slepton masses.

	BLRSP1	BLRSP2	BLRSP3	BLRSP4	BLRSP5
Sneutrinos and Sleptons					
$m_{\tilde{\nu}_1}$ [GeV]	102.3 ($\tilde{\nu}_R$)	797.0 ($\tilde{\nu}_R$)	91.6 ($\tilde{\nu}_R, \tilde{\nu}_L$)	542.3 ($\tilde{\nu}_R, \tilde{\nu}_L$)	753.4 ($\tilde{\nu}_R, \tilde{\nu}_L$)
$m_{\tilde{\nu}_2}$ [GeV]	102.3 ($\tilde{\nu}_R$)	797.0 ($\tilde{\nu}_R$)	92.6 ($\tilde{\nu}_R, \tilde{\nu}_L$)	542.3 ($\tilde{\nu}_R, \tilde{\nu}_L$)	753.9 ($\tilde{\nu}_R, \tilde{\nu}_L$)
$m_{\tilde{\nu}_3}$ [GeV]	203.0 ($\tilde{\nu}_R$)	797.0 ($\tilde{\nu}_R$)	92.6 ($\tilde{\nu}_R, \tilde{\nu}_L$)	542.3 ($\tilde{\nu}_R, \tilde{\nu}_L$)	753.9 ($\tilde{\nu}_R, \tilde{\nu}_L$)
$m_{\tilde{\nu}_4}$ [GeV]	573.8 ($\tilde{\nu}_R$)	1120.1 ($\tilde{\nu}_R, \tilde{\nu}_L$)	253.4 ($\tilde{\nu}_L, \tilde{\nu}_R$)	585.4 ($\tilde{\nu}_L, \tilde{\nu}_R$)	785.5 ($\tilde{\nu}_L, \tilde{\nu}_R$)
$m_{\tilde{\nu}_{5,6}}$ [GeV]	604.4 ($\tilde{\nu}_R$)	1120.3 ($\tilde{\nu}_R, \tilde{\nu}_L$)	258.2 ($\tilde{\nu}_L, \tilde{\nu}_R$)	586.7 ($\tilde{\nu}_L, \tilde{\nu}_R$)	789.0 ($\tilde{\nu}_L, \tilde{\nu}_R$)
$m_{\tilde{\nu}_7}$ [GeV]	725.2 ($\tilde{\nu}_L$)	1220.0 ($\tilde{\nu}_L, \tilde{\nu}_R$)	1374.0 ($\tilde{\nu}_L, \tilde{\nu}_R$)	953.4 ($\tilde{\nu}_R$)	950.1 ($\tilde{\nu}_R$)
$m_{\tilde{\nu}_{8,9}}$ [GeV]	734.1 ($\tilde{\nu}_L$)	1236.6 ($\tilde{\nu}_L, \tilde{\nu}_R$)	1374.0 ($\tilde{\nu}_R$)	953.4 ($\tilde{\nu}_R$)	950.1 ($\tilde{\nu}_R$)
$m_{\tilde{e}_1}$ [GeV]	484.1 ($\tilde{\tau}_R$)	1013.9 ($\tilde{\tau}_R$)	254.7 ($\tilde{\tau}_L, \tilde{\tau}_R$)	263.0 ($\tilde{\tau}_R$)	580.4 ($\tilde{\tau}_R$)
$m_{\tilde{e}_{2,3}}$ [GeV]	512.7 ($\tilde{\mu}_R$)/(\tilde{e}_R)	1055.3 ($\tilde{\mu}_R$)/(\tilde{e}_R)	265.6 ($\tilde{\mu}_L$)/(\tilde{e}_L)	270.5 ($\tilde{\mu}_R$)/(\tilde{e}_R)	592.3 ($\tilde{\mu}_R$)/(\tilde{e}_R)
$m_{\tilde{e}_4}$ [GeV]	732.1 ($\tilde{\tau}_L$)	1222.4 ($\tilde{\tau}_L$)	447.7 ($\tilde{\tau}_R, \tilde{\tau}_L$)	591.6 ($\tilde{\tau}_L$)	788.0 ($\tilde{\tau}_L$)
$m_{\tilde{e}_{5,6}}$ [GeV]	738.8 ($\tilde{\mu}_L$)/(\tilde{e}_L)	1237.9 ($\tilde{\mu}_L$)/(\tilde{e}_L)	450.6 ($\tilde{\mu}_R$)/(\tilde{e}_R)	592.2 ($\tilde{\mu}_L$)/(\tilde{e}_L)	790.9 ($\tilde{\mu}_L$)/(\tilde{e}_L)
Squarks					
$m_{\tilde{u}_1}$ [GeV]	1144.0 (\tilde{t}_R, \tilde{t}_L)	1185.4 (\tilde{t}_R, \tilde{t}_L)	1247.0 (\tilde{t}_R, \tilde{t}_L)	1111.3 (\tilde{t}_R, \tilde{t}_L)	1316.0 (\tilde{t}_R, \tilde{t}_L)
$m_{\tilde{u}_2}$ [GeV]	1392.1 (\tilde{t}_L, \tilde{t}_R)	1851.9 (\tilde{t}_L, \tilde{t}_R)	1526.9 (\tilde{t}_L, \tilde{t}_R)	1361.4 (\tilde{t}_L, \tilde{t}_R)	1643.2 (\tilde{t}_L, \tilde{t}_R)
$m_{\tilde{u}_{3,4}}$ [GeV]	1456.0 (\tilde{c}_R)/(\tilde{u}_R)	2154.7 (\tilde{c}_R)/(\tilde{u}_R)	1565.9 (\tilde{c}_R)/(\tilde{u}_R)	1392.4 (\tilde{c}_R)/(\tilde{u}_R)	1728.0 (\tilde{c}_R)/(\tilde{u}_R)
$m_{\tilde{u}_{5,6}}$ [GeV]	1509.0 [\tilde{c}_L, \tilde{u}_L]	2227.3 [\tilde{c}_L, \tilde{u}_L]	1634.0 [\tilde{c}_L, \tilde{u}_L]	1448.8 [\tilde{c}_L, \tilde{u}_L]	1795.8 [\tilde{c}_L, \tilde{u}_L]
$m_{\tilde{d}_1}$ [GeV]	1359.2 (\tilde{b}_L, \tilde{b}_R)	1819.2 (\tilde{b}_L)	1409.8 (\tilde{b}_R, \tilde{b}_L)	1326.3 (\tilde{b}_L)	1611.8 (\tilde{b}_L)
$m_{\tilde{d}_2}$ [GeV]	1464.0 (\tilde{b}_R, \tilde{b}_L)	2148.1 (\tilde{b}_R)	1462.3 (\tilde{s}_R)	1420.1 (\tilde{b}_R)	1724.5 (\tilde{b}_R)
$m_{\tilde{d}_3}$ [GeV]	1489.8 (\tilde{s}_R)	2175.9 (\tilde{s}_R)	1462.3 (\tilde{d}_R)	1426.2 (\tilde{s}_R)	1734.8 (\tilde{s}_R)
$m_{\tilde{d}_4}$ [GeV]	1489.8 (\tilde{d}_R)	2175.9 (\tilde{d}_R)	1496.2 (\tilde{b}_L, \tilde{b}_R)	1426.2 (\tilde{d}_R)	1734.8 (\tilde{d}_R)
$m_{\tilde{d}_{5,6}}$ [GeV]	1509.0 [\tilde{s}_L, \tilde{d}_L]	2228.9 [\tilde{s}_L, \tilde{d}_L]	1635.9 [\tilde{s}_L, \tilde{d}_L]	1450.9 [\tilde{s}_L, \tilde{d}_L]	1795.8 [\tilde{s}_L, \tilde{d}_L]
Neutralinos					
$m_{\chi_1^0}$ [GeV]	282.2 (\tilde{B})	416.7 (\tilde{B})	312.9 (\tilde{B})	258.5 (\tilde{h}_R)	346.6 (\tilde{B})
$m_{\chi_2^0}$ [GeV]	552.3 (\tilde{W}, \tilde{h}_L)	780.0 (\tilde{h}_R)	615.3 (\tilde{W}, \tilde{h}_L)	279.7 (\tilde{B})	679.5 (\tilde{W}, \tilde{h}_L)
$m_{\chi_3^0}$ [GeV]	828.9 (\tilde{h}_L)	817.5 (\tilde{W})	1086.6 (\tilde{h}_L)	549.0 (\tilde{W}, \tilde{h}_L)	902.7 (\tilde{h}_R)
$m_{\chi_4^0}$ [GeV]	838.9 (\tilde{h}_L, \tilde{W})	1865.5 (\tilde{h}_L)	1092.8 (\tilde{h}_L, \tilde{W})	844.9 (\tilde{h}_L)	1133.1 (\tilde{h}_L)
$m_{\chi_5^0}$ [GeV]	1230.4 ($\tilde{B}_\perp, \tilde{h}_R$)	1865.7 (\tilde{h}_L)	1232.2 ($\tilde{h}_R, \tilde{B}_\perp$)	856.8 (\tilde{h}_L, \tilde{W})	1139.4 (\tilde{h}_L, \tilde{W})
$m_{\chi_6^0}$ [GeV]	1650.9 (\tilde{h}_R)	2017.6 ($\tilde{B}_\perp, \tilde{h}_R$)	1811.3 ($\tilde{B}_\perp, \tilde{h}_R$)	1639.0 ($\tilde{B}_\perp, \tilde{h}_R$)	1489.8 ($\tilde{B}_\perp, \tilde{h}_R$)
$m_{\chi_7^0}$ [GeV]	2608.3 ($\tilde{h}_R, \tilde{B}_\perp$)	2392.3 ($\tilde{h}_R, \tilde{B}_\perp$)	2741.4 ($\tilde{h}_R, \tilde{B}_\perp$)	2174.6 ($\tilde{h}_R, \tilde{B}_\perp$)	2056.5 ($\tilde{h}_R, \tilde{B}_\perp$)

TABLE III: Susy spectra of our study points, for discussion see text. ($\tilde{\nu}_R$) is a nearly maximal mixture of the right sneutrinos and the S -fields.

	BLRSP1	BLRSP2	BLRSP3	BLRSP4	BLRSP5
Light higgses (1-loop/2-loop)					
m_{h_1} [GeV]	59.1/59.6	119.2/125.4	92.7/93.1	100.8/102.6	18.8/18.8
m_{h_2} [GeV]	119.0/124.1	139.7/140.4	114.5/120.1	121.0/124.8	115.7/121.8
\mathcal{R}_{L1}^2	0.05/0.04	0.90/0.83	0.07/0.04	0.33/0.22	0.001/0.001
\mathcal{R}_{L2}^2	0.95/0.96	0.10/0.17	0.93/0.96	0.67/0.78	0.999/0.999
Heavy scalars/pseudoscalars					
m_{h_3} [GeV]	971.5	2176.5	1268.2	948.2	1345.6
m_{h_4} [GeV]	5074.9	7883.3	2268.2	3024.7	2227.2
m_{A_1} [GeV]	972.8	2177.5	796.3	949.2	1346.8
m_{A_2} [GeV]	4789.4	7581.1	1269.3	2345.1	1477.8

TABLE IV: Higgs spectra of our study points, for discussion see text.

A. Lepton decays and LFV

To explain the measured neutrino mixing angles by the mass matrix given in eq. (39) the Yukawa couplings Y_ν , Y_s and/or the bilinear term μ_S have to contain off-diagonal elements. In case that the neutrino mixing is explained by the form of Y_ν or Y_s also lepton flavor violation in the charged lepton sector will be induced. On the one hand the contributions of Y_ν to the RGE evaluation branching ratios of Y_e and to the soft-breaking terms in the lepton sector open decay channels like $l_i \rightarrow l_j \gamma$ and $l_i \rightarrow 3l_j$ similarly to high-scale seesaw type I–III [84–86]. On the other hand, in inverse seesaw the entries of Y_ν can be potential large and the dominant contributions to LFV decays can come from diagrams which are proportional to $(Y_\nu Y_\nu^\dagger)_{ij}$. For a long time it has been assumed that the most stringent bounds on $(Y_\nu Y_\nu^\dagger)_{ij}$ come from the radiative decay $\mu \rightarrow e \gamma$ while the photonic contributions to $\mu \rightarrow 3e$ are always smaller and therefore $\text{Br}(\mu \rightarrow e \gamma) > \text{Br}(\mu \rightarrow 3e)$ must hold. However, recently it has been pointed out that in presence of new Yukawa couplings like Y_ν the Z -penguin contributions to $\text{Br}(\mu \rightarrow 3e)$ can dominate [87]. These are less suppressed than the photonic contributions by a factor $\left(\frac{M_{SUSY}}{M_Z}\right)^4$. As consequence, the experimental limits on the decay into two charged electrons can be much more constraining than the radiative decay in case of a heavy SUSY spectrum. We can see this by parametrizing the neutrino Yukawa coupling as

$$Y_\nu = f \begin{pmatrix} 0 & 0 & 0 \\ a & a & -a \\ b & 1 & 1 \end{pmatrix}, \quad (48)$$

with

$$a = (\Delta m_\odot^2 / \Delta m_A^2)^{\frac{1}{4}} \sim 0.4 \quad \text{and} \quad b = 0.23. \quad (49)$$

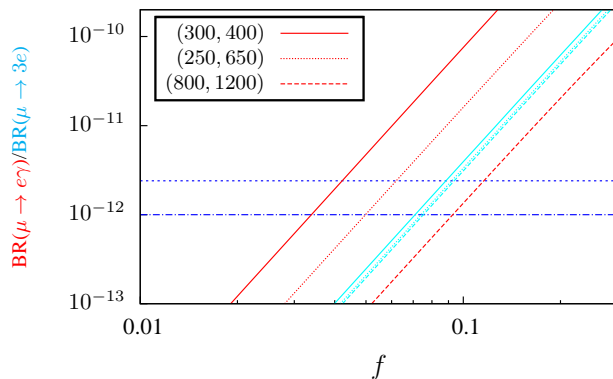


FIG. 9: Branching ratios of lepton flavour violating processes as a function of f for $\tan\beta = 10$, $A_0 = 0$, $v_R = 5000$ GeV, $\tan\beta_R = 1.05$, $\mu_R = -500$ GeV, $m_{A_R} = 1000$ GeV and three $(m_0, M_{1/2})$ combinations. The dashed blue line is the upper limit for $\mu \rightarrow e\gamma$ and the dashed-dotted blue line for $\mu \rightarrow 3e$.

Here, Δm_{\odot}^2 and Δm_{A}^2 are the mass differences measured in solar and atmospheric neutrino oscillations. The value of b accommodates for $\sin^2\theta_{13} = 0.026$.

$\text{Br}(\mu \rightarrow e\gamma)$ and $\text{Br}(\mu \rightarrow 3e)$ as function of f are depicted in fig. 9, and we show also the most recent, experimental limits of [51, 88]

$$\text{Br}(\mu \rightarrow e\gamma) < 2.4 \cdot 10^{-12}, \quad \text{Br}(\mu \rightarrow 3e) < 1.0 \cdot 10^{-12} \quad (50)$$

For the plot we chose three different points for $(m_0, M_{1/2})$. Since $\text{Br}(\mu \rightarrow 3e)$ hardly depends on SUSY masses for $m_{\text{SUSY}} \gg m_Z$ all three lines lie very close together in contrast to $\text{Br}(\mu \rightarrow e\gamma)$. For light SUSY spectra $\text{Br}(\mu \rightarrow e\gamma)$ is dominant whereas the heavier the SUSY particles the more important gets $\text{Br}(\mu \rightarrow 3e)$. As shown in BLRSP1 and BLRSP2 we can have light right-handed neutrinos such that contributions from the W -graph to LFV can not be neglected anymore. In fig. 10 $\text{Br}(\mu \rightarrow e\gamma)$ and $\text{Br}(\mu \rightarrow 3e)$ are plotted as a function of m_{ν_R} . For masses below 300 GeV contributions from right-handed neutrinos start to dominate. The minimum in $\text{Br}(\mu \rightarrow 3e)$ comes from a cancelation between the right-handed neutrino and the corresponding SUSY graph. In the limit of large m_{ν_R} $\text{Br}(\mu \rightarrow e\gamma)$ and $\text{Br}(\mu \rightarrow 3e)$ converge to the value coming from SUSY contributions.

However, it is possible to circumvent these bounds by assuming that Y_ν and Y_s are diagonal and the entire neutrino mixing is explained by μ_S . Of course, this will not only reduce $\text{Br}(\mu \rightarrow 3e)$ but also $\text{Br}(\mu \rightarrow e\gamma)$.

B. Higgs physics, direct production

In all study points of table II there is one Higgs boson with mass between 120 and 125 GeV. In addition, there is a second state with masses varying between 19 and 140 GeV. In BLRSP1, BLRSP3 and BLRSP5 the mass eigenstate h_2 is SM-like, with $R_{L2}^2 > 0.9$. In

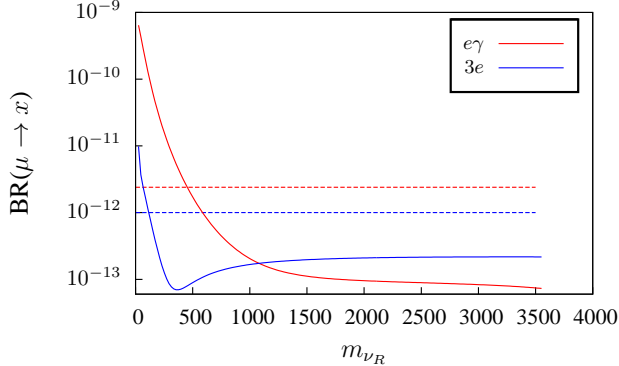


FIG. 10: Branching ratios of lepton flavour violating processes as a function of m_{ν_R} for $m_0 = 800$ GeV, $M_{1/2} = 1200$ GeV, $\tan \beta = 10$, $A_0 = 0$, $v_R = 10$ TeV, $\tan \beta_R = 1.05$, $\mu_R = -500$ GeV, $m_{A_R} = 1000$ GeV. The dashed red line is the upper limit for $\mu \rightarrow e\gamma$ and the dashed blue line for $\mu \rightarrow 3e$.

BLRSP2 it is h_1 , which has a large content of H_d and H_u and BLRSP4 is a case where h_1 and h_2 have large mixing. Since we have often a mass eigenstate below the LEP limit of 115 GeV for a standard model Higgs boson, we have checked the consistency of these eigenstates with data using `HiggsBounds 3.4.0beta` [89, 90]. All points are allowed by accelerator constraints, but sometimes very close to existing bounds, especially BLRSP4 and also BLRSP2. As an indication for the theoretical uncertainties in the mass calculation we give the masses using the complete 1-loop formulas and the ones adding the dominant 2-loop corrections to the MSSM sector [91–96].

In BLRSP1 and BLRSP5 h_1 is so light that the decay $h_2 \rightarrow h_1 h_1$ is kinematically allowed. However, the mixing between both sectors is so small that for BLRSP1 the corresponding branching ratio is about 1 per-cent whereas for BLRSP5 it is a few per-mile. The smallness of this decay is a direct consequence of the bounds imposed by LEP and the decay $h_2 \rightarrow h_1 h_1$ can never be dominant in the BLR model. The h_2 can also decay into a combination of heavy and light neutrinos with a branching ratio of a few per-cent, as for example in case of BLRSP1 leading to the final states

$$h_2 \rightarrow \nu_i \nu_k \rightarrow \nu_i l^\pm W^\mp \quad (51)$$

$$h_2 \rightarrow \nu_i \nu_k \rightarrow \nu_i \nu_j Z \quad (52)$$

with $i, j = 1, 2, 3$ and $k = 4, \dots, 9$. These final states can also be obtained via intermediate states containing an off-shell vector boson, e.g. WW^* and ZZ^* . However, their existence implies that ratio of quark versus lepton final states will not correspond to the branching ratios of the vector bosons. Note, however, that for hadronic W-boson decays the invariant mass of jj +lepton system would show a peak at the heavy neutrino mass, which allows to identify this signature, in principle. Apart from these decays, the h_2 can also decay to two scalar neutrinos and, if kinematically allowed, this decay can become dominant, leading to

a (nearly) invisible Higgs boson.

The hint for a 125 GeV Higgs boson [7, 8], see also [44] and [45], indicates a slightly larger than expected branching ratio into the two-photon final state. In [18] it was shown that the NMSSM can, in principle, explain such an enhanced di-photon rate, due to a possible mixing of the singlet and the Higgs, which reduces the coupling of the Higgs to bottom quarks, thus reducing the total width, without affecting the production cross section. In the case of the BLR model, such a construction is not possible, since our singlets are charged under $U(1)_R$ and the mixing between SM and BLR sectors is controlled by $\tan\beta_R$. Since we have to choose $\tan\beta_R$ close to one, the singlets mix to the up and down components of the Higgs equally. Therefore a reduction of $h \rightarrow b\bar{b}$ causes a reduction of the coupling for gluon fusion as well. Thus, a sizeable enhancement of $\text{Br}(h \rightarrow \gamma\gamma)$ by reducing simply the total width is not possible in the BLR model. Currently the discrepancy of the data with expectations is only at the level of about 1σ c.l. However, should future data show indeed an enhanced rate for the $\gamma\gamma$ final state, this would be hard to explain in the BLR model.

In the four points (BLRSP1, BLRSP3-BLRSP5) h_1 has approximately the same branching ratios for the decays into SM-fermions as a SM Higgs boson of the same mass. However, the corresponding widths are suppressed by the mixing with the usual MSSM sector which reduces the width by a factor between 10^2 and 10^4 . At the LHC the main production of this particle is via SUSY cascade decays, e.g. it appears in the decays of $\tilde{\nu}_{4,5,6}$ (BLRSP1, BLRSP3), $\tilde{\chi}_3^0$ (BLRSP4) or in the decays of the heavy neutrinos which are produced via the Z' (BLRSP1, BLRSP4) as discussed in section V. However, in case of BLRSP5 LHC will miss h_1 as it only appears in the decays of the heavy Higgs bosons which have masses in the TeV range.

Study point BLRSP2 differs from the others as here h_1 is the MSSM-like Higgs boson and h_2 has a mass of 140 GeV which could explain the slight excess in this region observed by ATLAS and CMS in the early data [97, 98]. In this region of the parameter space the Higgs at 125 GeV is made as in the MSSM, implying a rather heavy SUSY spectrum. This is due to the fact that a 140 GeV Higgs with reduced couplings can only be the h_{BLR} , i.e. this points exist to the right of the level-crossing region shown in fig. 2. Due to the choice of a rather small Y_s in this point the heavy neutrinos masses are below the mass of h_2 . This leads to non-standard decays into the heavy neutrinos which dominantly decay to a lepton and a W-boson.

C. Z' physics

As already mentioned in sect. III A, our Z' corresponds essentially to the Z_χ in the notation of [80]. In previous studies usually two assumptions have been made in the construction of mass bounds: (i) the Z' decays only into the known SM particles [99] and (ii) the effects of gauge kinetic mixing are neglected. Both assumptions are not truly valid in the BLR model. For a recent study of Z' bounds without these assumptions see [100]. As shown in table V we find in all our points that the heavy neutrinos appear as final states beside the

TABLE V: Branching ratios of the dominant Z' decay modes. Here we have summed over the generations in case of the charged fermions and sfermions. For the neutrinos we have splitted this sum into a sum over the light (heavy) states denoted by ν_l (ν_h).

final state	BLRSP1	BLRSP2	BLRSP3	BLRSP4	BLRSP5
$BR(dd)$	0.31	0.35	0.35	0.37	0.43
$BR(uu)$	0.06	0.07	0.07	0.07	0.08
$BR(ll)$	0.12	0.14	0.14	0.14	0.16
$BR(\nu_l\nu_l)$	0.10	0.11	0.12	0.12	0.12
$BR(\nu_h\nu_h)$	0.27	0.30	0.13	0.11	0.13
$BR(\tilde{\nu}\tilde{\nu})$	0.05	—	0.05	0.03	—
$BR(\tilde{l}\tilde{l})$	—	—	0.05	0.03	—
$BR(\tilde{\chi}_2^+\tilde{\chi}_2^-)$	—	—	—	0.02	—
$BR(\tilde{\chi}_4^0\tilde{\chi}_5^0)$	—	—	—	0.02	—

	c_L	c_R
d	$-\frac{i}{6}(-3g_L Z^{13} + g_{BL} Z^{23} + g_{BLR} Z^{33})$	$-\frac{i}{6}((g_{BL} - 3g_{RBL})Z^{23} + (g_{BLR} - 3g_R)Z^{33})$
u	$-\frac{i}{6}(3g_L Z^{13} + g_{BL} Z^{23} + g_{BLR} Z^{33})$	$-\frac{i}{6}((g_{BL} + 3g_{RBL})Z^{23} + (g_{BLR} + 3g_R)Z^{33})$
l	$\frac{i}{2}(g_L Z^{13} + g_{BL} Z^{23} + g_{BLR} Z^{33})$	$\frac{i}{2}((g_{BL} + g_{RBL})Z^{23} + (g_{BLR} + g_R)Z^{33})$
ν	$\frac{i}{2}\left[\sum_{x=1}^3 Z_\nu^{j^{3+x,*}} Z_\nu^{i^{3+x}}((-g_{BL} + g_{RBL})Z^{23} + (g_R - g_{BLR})Z^{33}) + \sum_{x=1}^3 Z_\nu^{j^{x,*}} Z_\nu^{i^x}(g_{BL} Z^{23} - g_L Z^{13} + g_{BLR} Z^{33})\right]$	$-\frac{i}{2}\left[\sum_{x=1}^3 Z_\nu^{i^{3+x,*}} Z_\nu^{j^{3+x}}((-g_{BL} + g_{RBL})Z^{23} + (g_R - g_{BLR})Z^{33}) + \sum_{x=1}^3 Z_\nu^{i^{x,*}} Z_\nu^{j^x}(g_{BL} Z^{23} - g_L Z^{13} + g_{BLR} Z^{33})\right]$

TABLE VI: Coefficients c_L^f and c_R^f for the coupling between Z_R and two leptons or quarks. Here, Z is the rotation matrix diagonalizing the neutral gauge boson mass matrix and Z_ν is the neutrino mixing matrix.

SM-fermions. Moreover, in all but BLRSP5 also supersymmetric particles appear as decay products, in particular sneutrinos and sleptons. On the other hand, gauge kinetic effects are in this model less important and were only important if one could measure the branching with a precision of 1 per-cent or better.

The Z' couples to leptons and quarks as follows

$$Z'_\mu \bar{f} \gamma^\mu (c_L^f P_L + c_R^f P_R) f \quad (53)$$

The different coefficients are given in table VI.

Note, that in the couplings to the u -quarks a partial cancellation occurs in contrast to the ones to d -quarks, which get enhanced. Moreover, the same feature appears in the vertex $\tilde{q}-q-\tilde{B}_\perp$ which leads to some interesting consequences discussed in section IV E.

We find that the decays into the heavy neutrino states are always possible and have a sizable branching ratio provided $\text{Tr}(|Y_s|) \lesssim 1$. In table V we summarize the most important final states of the Z' for the different scenarios. As can be seen the heavy neutrino final

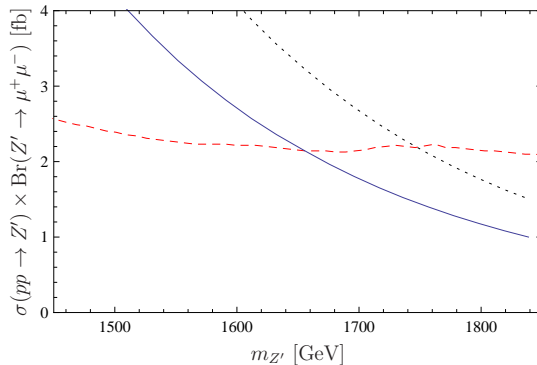


FIG. 11: Cross section of $pp \rightarrow Z' \rightarrow \mu^+ \mu^-$ near the Z' peak as function of $m_{Z'}$ taking into account a K-factor of 1.3 [106]. For the black, dotted line the Z' width has been calculated allowing only SM final states, while the blue solid includes also right-handed neutrinos and SUSY states. The red line shows the ATLAS exclusion limit [79]. We have used as input BLRSP1 and varied $v_R = [4.1, 5.1]$ TeV.

states have always a sizable branching ratios with up to about 30 per-cent when summing over the generations. But even for rather heavy neutrinos as in BLRSP5 own finds for this channel a 15 per-cent branching ratio. In several cases also channels into SUSY particles are open, in particular in scenarios with sneutrino LSPs. In case of supersymmetric particles the final states containing sleptons or sneutrinos have the largest branching ratios. Channels into neutralinos or charginos are suppressed. They proceed either via the mixing with the Z which is rather small or via the projection of the higgsino-right onto the corresponding neutralino state.

The appearance of additional final states leads to a reduction of the event numbers in the most sensitive search channels, i.e. reducing cross section times branching ratio, and, thus, the bounds obtained by the LHC collaborations [79, 101, 102] are less constraining in the BLR model. This is depicted in fig. 11 where we show the production cross section $\sigma(pp \rightarrow \mu^+ \mu^-)$ around the Z' resonance.⁸ In case that the width of the Z' is calculated using only SM final states the cross section is increased roughly by a factor 1.6 in comparison to the case where also right handed neutrinos and SUSY particle contribute to the width of Z' . With this choice of parameters, the main effect is due to R-neutrinos. We attribute the remaining difference to the official ATLAS result to slightly different values in the couplings and slightly different branching ratios of the final states. Our results agree also with the ones of ref. [80]. We conclude that, although in our benchmark points we take always $m_{Z'} > 1.8$ TeV, a significantly lower mass is possible consistent with data.

⁸ For the calculation of the cross section we used WHIZARD [103, 104] and implemented the model using the SUSY Toolbox [105].

D. Heavy neutrinos

As discussed above, the heavy neutrino states can be produced via the Z' with a considerable branching ratio of about 30 per-cent when summing over all heavy neutrinos. Moreover, see below, they can also be produced in the cascade decays of supersymmetric particles. These heavy neutrinos mix with the light neutrino states implying a reduction of the couplings of the light neutrinos to the Z -boson and, thus, also a reduction of the invisible width of the Z -boson. Taking the data from ref. [51] this can be translated into the following condition on the 3×3 sub-block U_{ij}^ν , $i, j \leq 3$, of the neutrino mixing matrix:

$$\left| 1 - \sum_{ij=1, i \leq j}^3 \left| \sum_{k=1}^3 U_{ik}^\nu U_{jk}^{\nu,*} \right|^2 \right| < 0.009 \quad (54)$$

at the $3\text{-}\sigma$ level. We have checked that all our benchmark points fulfill this condition.

The main decay modes of the heavy neutrinos are⁹

$$\nu_j \rightarrow W^\pm l^\mp \quad (55)$$

$$\nu_j \rightarrow Z \nu_i \quad (56)$$

$$\nu_j \rightarrow h_k \nu_i \quad (57)$$

where $j \geq 4$, $i \leq 3$, $k = 1, 2$ and $l = e, \mu, \tau$, provided they are kinematically allowed. If there is no kinematical suppression we find in general the branching ratios scale like $BR(\nu_j \rightarrow W^\pm l^\mp) : BR(\nu_j \rightarrow Z \nu_i) : BR(\nu_j \rightarrow h_k \nu_i) \simeq 0.5 : 0.25 : 0.25$ where we have summed over the light Higgs bosons, the light neutrinos and leptons, respectively. We stress that these states are quasi-Dirac neutrinos and, thus, for six heavy neutrinos at LHC the existence of up to three new particles could be established. Note, that the final states containing a W -boson allow for a direct mass measurement.

Beside the above decay modes, also decays into SUSY particle are possible if kinematics allow for it. For example we find that for BLRSP4 the decay into $\tilde{\nu}_{1,2,3} \tilde{\chi}_1^0$ are possible and have branching ratios of about 3 per-cent. In scenarios like BLRSP3, BLRSP4 and BLRSP5 the main production of the heavy neutrinos is via the Z' and, thus, a high luminosity will be required to observe such final states.

E. SUSY cascade decays

In this section we point out several features which distinguish the BLR model from the usual MSSM. For the sake of preparing the ground, let us first summarize the main features of the MSSM relevant for the LHC, focusing for the time being on scenarios where the gluino is heavier than the squarks: (i) The gluino decays dominantly into squarks and quarks. (ii)

⁹ For related discussions see e.g. [107–109] and references therein.

L-squarks and L-sleptons decay dominantly into the chargino and the neutralino which are mainly $SU(2)_L$ -gauginos. Apart from kinematical effects the branching ratio for decays into the charged wino divided by the branching ratio into the neutral wino is about 2:1. (iii) R-squarks and R-sleptons decay dominantly into the bino-like neutralino with a branching ratio often quite close to 100 per-cent. (iv) In case of third generation sfermions also decays into higgsinos are important.

In the BLR model one has two main new features: (i) there are additional neutralinos and (ii) the sneutrino sector is enlarged as well. The latter implies that sneutrino LSPs are possible consistent with all astrophysical constraints and direct dark matter searches [110–116]. This feature is for example realised in study points BLRSP1 and BLRSP3¹⁰.

Let us start the discussion with BLRSP1. In this point the four lighter neutralinos are the usual MSSM neutralinos with the standard hierarchy. The fifth state corresponds to the additional $U(1)$ -gaugino, which we call \tilde{B}_\perp , whereas the two additional states are the additional higgsinos. Note that the lightest neutralino is not stable anymore but decays into final states containing all nine neutrinos as well as the three lightest sneutrinos. Of the latter ones the second lightest is so long lived that it will lead to a displaced vertex in a typical collider detector. The third sneutrino decays dominantly via three-body decays into $l^+l^-\tilde{\nu}_i$ and $\nu_k\nu_l\tilde{\nu}_i$ with $i = 1, 2$ and $k, l = 1, 2, 3$. As discussed in section IVD the heavy neutrinos decay dominantly into W -bosons and charged leptons, thus the decays of the lightest neutralino are not invisible.

\tilde{B}_\perp appears for example in the decays of \tilde{d}_R and \tilde{s}_R with branching ratios $\text{BR}(q\tilde{\chi}_1^0) \simeq 0.8$ and $\text{BR}(q\tilde{\chi}_5^0) \simeq 0.2$. For completeness we remark that the decays of \tilde{u}_R and \tilde{c}_R into $\tilde{\chi}_5^0$ is suppressed as the corresponding coupling is suppressed as are the couplings of Z' to u -type quarks in this model. $\tilde{\chi}_5^0$ decays dominantly into sleptons and sneutrinos. Combining all the above together one gets a much richer structure for the decays of the R-squarks, e.g. the following decay chains:

$$\tilde{q}_R \rightarrow q\tilde{\chi}_1^0 \rightarrow q\nu_k\tilde{\nu}_1 \rightarrow q\nu_j Z\tilde{\nu}_1 \quad (58)$$

$$\tilde{q}_R \rightarrow q\tilde{\chi}_1^0 \rightarrow q\nu_k\tilde{\nu}_1 \rightarrow ql^\pm W^\mp\tilde{\nu}_1 \quad (59)$$

$$\tilde{q}_R \rightarrow q\tilde{\chi}_1^0 \rightarrow q\nu_k\tilde{\nu}_3 \rightarrow ql^\pm W^\mp\tilde{l}'^+l'^-\nu_1 \quad (60)$$

$$\tilde{q}_R \rightarrow q\tilde{\chi}_5^0 \rightarrow ql^\pm\tilde{l}_i^\mp \rightarrow ql^\pm l^\mp\tilde{\chi}_1^0 \rightarrow ql^\pm l^\mp\nu_k\tilde{\nu}_1 \rightarrow ql^\pm l^\mp l'^\pm W^\mp\tilde{\nu}_1 \quad (61)$$

with $k \in \{4, 5, 6, 7, 8, 9\}$ and $j \in \{1, 2, 3\}$. Of course, several other combinations are possible as well.

From equations (58) to (61) one sees immediatly that the standard signature of R-squarks, namely jet and missing energy, is only realized in a few cases in this study point, e.g. if in eq. (58) the Z decays into neutrinos. Interestingly, the chain via $\tilde{\chi}_5^0$ into sleptons leads to a characteristic edge in the invariant mass of the lepton which can be used to determine

¹⁰ We note for completeness, that the relic abundance is actually somewhat too large in this point but can easily be adjusted by changing for example in BLRSP1 $\tan\beta_R$ from 1.05 to 1.0475 without changing the collider features of BLRSP1.

the corresponding masses once combined with information from other decay chains. Also in the study points BLRSP2 and BLRSP5 \tilde{d}_R and \tilde{s}_R decay into heavy neutralinos, which contain sizable content of the extra $U(1)$ gaugino, with a sizable branching ratio. However, there the situation is somewhat less involved as in these study points the lightest bino-like neutralino is the LSP.

Another interesting feature is, that $\tilde{\chi}_5^0$ decays also into the heavier sneutrinos which themselves decay into the LSP plus h_1 . Similarly h_1 can be produced in the decays of the heavy neutrinos implying that this state can be produced with sizable rate in SUSY cascade decays. However, as the corresponding final states are quite complicated a dedicated Monte Carlo study will be necessary to decide if this is indeed a discovery channel for h_1 .

From the point of view of SUSY cascade decays BLRSP2 looks essentially like a standard MSSM point. Inspection of the spectrum shows that $\tilde{\chi}_2^0$ is essentially a higgsino corresponding to the extended $U(1)$ sector but it shows hardly up in the cascade decays. Its main production channel is via an s -channel Z' but even in this case the corresponding cross section is so low that it will not be detected at the LHC even with an integrated luminosity of 300 fb^{-1} . Another interesting feature shows up in the decays of $\tilde{\chi}_3^0$ which is mainly the neutral wino and gets copiously produced in the decays of the L-squarks: it decays with about 77 (15) per-cent into h_1 (h_2), implying that the cascade decays are an important source of Higgs bosons.

In case of BLRSP3 one has sneutrino LSPs like in BLRSP1 but with a different hierarchy in the spectrum, as the three lightest sleptons are lighter than the highest neutralino. Therefore the $\tilde{\chi}_1^0$ has also sizable decay rates into charged sleptons which sum to about 30 per-cent. The sleptons decay then further into $W^- \tilde{\nu}_{1,2,3}$ and $\nu_{2,3}$ via 3-body decays into $f\bar{f}$ -pairs. The latter, however, are rather soft due to the small mass difference. In addition we have the decay channel into a light neutrino and one of the heavier sneutrinos which themselves decay into a lighter sneutrino and either one of the Higgs boson or the Z -boson. Putting again all these decays together one obtains for the $\tilde{\chi}_1^0$ decays

$$\tilde{\chi}_1^0 \rightarrow l^\pm \tilde{l}^\mp \rightarrow l^\pm W^\mp \tilde{\nu}_1 \quad (62)$$

$$\tilde{\chi}_1^0 \rightarrow l^\pm \tilde{l}^\mp \rightarrow l^\pm W^\mp \tilde{\nu}_{2,3} \rightarrow l^\pm W^\mp f \bar{f} \tilde{\nu}_1 \quad (63)$$

$$\tilde{\chi}_1^0 \rightarrow \nu_j \tilde{\nu}_{2,3} \rightarrow \nu_{1,2,3} f \bar{f} \tilde{\nu}_1 \quad (64)$$

$$\tilde{\chi}_1^0 \rightarrow \nu_j \tilde{\nu}_1 \quad (65)$$

$$\tilde{\chi}_1^0 \rightarrow \nu_j \tilde{\nu}_k \rightarrow \nu_j h_{1,2} \tilde{\nu}_1 \quad (66)$$

$$\tilde{\chi}_1^0 \rightarrow \nu_j \tilde{\nu}_k \rightarrow \nu_j h_{1,2} f \bar{f} \tilde{\nu}_1 \quad (67)$$

with $j = 1, 2, 3$ and $k = 4, 5, 6$. This implies that the decays of the R-squarks show again a more complicated structure compared to the usual CMSSM expectations. Channels (66) and (67) give h_1 in about 15 per-cent of the final states of $\tilde{\chi}_1^0$. Moreover, $\tilde{\chi}_2^0$ and $\tilde{\chi}_1^+$ decay dominantly into sleptons and sneutrinos. Here a new feature is found for $\tilde{\chi}_1^+$, as also the

following chains

$$\tilde{\chi}_1^+ \rightarrow l^+ \tilde{\nu}_{5,6} \rightarrow l^+ Z \tilde{\nu}_1 \quad (68)$$

$$\tilde{\chi}_1^+ \rightarrow l^+ \tilde{\nu}_{5,6} \rightarrow l^+ h_{1,2} \tilde{\nu}_1 \quad (69)$$

gives rise to sharp edge structures. However, as the main final states of Z and $h_{1,2}$ are two jets, the feasibility still needs to be investigated.

In BLRSP4 we have chosen $\mu_R = 260$ GeV in order to construct an LSP which is essentially a \tilde{h}_R . Here, the R -sleptons are lighter than $\tilde{\chi}_2^0$, which is essentially bino-like in this point, giving rise to the following decay chain of the down-type R -squarks

$$\tilde{d}_R \rightarrow d \tilde{\chi}_2^0 \rightarrow dl^\pm \tilde{l}^\mp \rightarrow dl^\pm l^\mp \tilde{\chi}_1^0 \quad (70)$$

Nearly all cascade decays end in a $\tilde{\chi}_2^0$ or one of the lighter sleptons. Due to the fact, that in this particular case the additional sneutrino states are hardly produced, it might be difficult to distinguish it from the NMSSM, at least as long as the Z' is not discovered. The heavier L -sleptons do not show up in the cascade decays of squarks and gluinos but can be produced via the Z' as discussed in section V.

BLRSP5 is similar to BLRSP1 but compatible with pure GUT conditions, e.g. μ_R and m_{A_R} are not input in this case but derived quantities. To fulfill the tadpole equations we have to choose $Y_s = 0.3$ and $\tan\beta_R = 1.03$ if we want a relatively low $m_0 = 500$ GeV while $M_{1/2} = 850$ GeV. The choice of Y_s leads automatically to large masses for the heavy neutrinos such that the lightest Higgs can not decay into those states. As in BLRSP1 the down-type R -squarks decay not only into $\tilde{\chi}_1^0$ but also into $\tilde{\chi}_6^0$ with a branching ratio of about 13 per-cent. For completeness, we note that here $\tilde{\chi}_3^0 \simeq \tilde{h}_R$. However this state gets hardly produced in any of the SUSY decays or via the Z' . Therefore, it is likely that LHC will miss it and also at a linear collider such as ILC or CLIC it will be difficult to study, due to the small production cross section.

V. CONCLUSIONS

We have studied the minimal supersymmetric $U(1)_{B-L} \times U(1)_R$ extension of the standard model. The model is minimal in the sense that the extended gauge symmetry is broken with the minimal number of Higgs fields. In the matter sector the model contains (three copies of) a superfield $\hat{\nu}^c$, to cancel anomalies. Adding three singlet superfields \hat{S} allows to generate small neutrino masses with an inverse seesaw mechanism.

The phenomenology of the model differs from the MSSM in a number of interesting aspects. We have focussed on the Higgs phenomenology and discussed changes in SUSY spectra and decays with respect to the MSSM. The model is less constrained than the CMSSM from the possible measurement of a Higgs with a mass of the order of 125 GeV. If the hints found in LHC data [7, 8] is indeed correct our model predicts two relatively light states should exist, with the second h^0 corresponding (mostly) to the lightest of the ‘‘right’’ Higgses, added to break the extended gauge group.

It is interesting, as we have discussed, that very often a right sneutrino is found to be the LSP. This will affect all constraints on CMSSM parameter space derived from constraints on the dark matter abundance. In fact, if the right sneutrino is indeed the LSP in our model, no constraint on any CMSSM parameters can be derived from DM constraints.

The model has new D-terms in all scalar mass matrices, which can lead to sizeable changes in the SUSY spectra, of potential phenomenological interest. We have discussed a few benchmark points, covering a number of features which could allow to distinguish the model from the CMSSM. Obviously this includes the discovery of a Z' at the LHC where we have shown that the current bounds from LHC data depend on the details of the particle spectrum. Also the cascade decays of supersymmetric particles can be significantly more involved than in the usual CMSSM as the additional neutralinos, neutrinos and sneutrinos lead to enhancement of the multiplicities in the final states. This implies that the existing limits on the CMSSM parameter space get modified as standard final states have reduced branching ratios and at the same time additional final states are present. In case that the mBLR model is indeed realized these new cascade decays will offer additional kinematical information on the particle spectrum.

Acknowledgments

W.P. thanks the IFIC for hospitality during an extended stay. M.H. and L.R. acknowledge support from the Spanish MICINN grants FPA2011-22975, MULTIDARK CSD2009-00064 and by the Generalitat Valenciana grant Prometeo/2009/091 and the EU Network grant UNILHC PITN-GA-2009-237920. L.R. thanks the Instituto Superior Técnico, Lisbon, for kind hospitality during an extended stay. W.P. has been supported by the Alexander von Humboldt foundation and in part by the DFG, project no. PO-1337/2-1 and the Helmholtz Alliance “Physics at the Terascale”.

Appendix A: Appendix

1. Mass matrices

Here we list the tree-level mass matrices of the model not given in the main text.

- **Mass matrix for Down-Squarks**, Basis: $(\tilde{d}_L, \tilde{d}_R)$

$$m_{\tilde{d}}^2 = \begin{pmatrix} m_{LL}^2 & \frac{1}{\sqrt{2}}(v_d T_d^\dagger - v_u \mu Y_d^\dagger) \\ \frac{1}{\sqrt{2}}(v_d T_d - v_u Y_d \mu^*) & m_{RR}^2 \end{pmatrix} \quad (\text{A1})$$

$$m_{LL}^2 = m_q^2 + \frac{v_d^2}{2} Y_d^\dagger Y_d - \frac{1}{24} \left((g_{BL}^2 + g_{BLR}^2 - g_{BLR}g_R - g_{BL}g_{RBL}) (v_{\chi_R}^2 - v_{\bar{\chi}_R}^2) + (3g_L^2 + g_{BL}g_{RBL} + g_{BLR}g_R) (v_d^2 - v_u^2) \right) \mathbf{1} \quad (\text{A2})$$

$$m_{RR}^2 = m_d^2 + \frac{v_d^2}{2} Y_d Y_d^\dagger + \frac{1}{24} \left((g_{BL}^2 + g_{BLR}^2 - 4(g_{BLR}g_R + g_{BL}g_{RBL}) + 3(g_R^2 + g_{RBL}^2)) (v_{\chi_R}^2 - v_{\bar{\chi}_R}^2) + (g_{BL}g_{RBL} + g_{BLR}g_R - 3(g_R^2 + g_{RBL}^2)) (v_d^2 - v_u^2) \right) \mathbf{1} \quad (\text{A3})$$

- **Mass matrix for Up-Squarks, Basis:** $(\tilde{u}_L, \tilde{u}_R)$

$$m_{\tilde{u}}^2 = \begin{pmatrix} m_{LL}^2 & \frac{1}{\sqrt{2}} (-v_d \mu Y_u^\dagger + v_u T_u^\dagger) \\ \frac{1}{\sqrt{2}} (-v_d Y_u \mu^* + v_u T_u) & m_{RR}^2 \end{pmatrix} \quad (\text{A4})$$

$$m_{LL}^2 = m_q^2 + \frac{v_u^2}{2} Y_u^\dagger Y_u - \frac{1}{24} \left((g_{BL}^2 + g_{BLR}^2 - g_{BLR}g_R - g_{BL}g_{RBL}) (v_{\chi_R}^2 - v_{\bar{\chi}_R}^2) + (3g_L^2 - g_{BL}g_{RBL} - g_{BLR}g_R) (v_u^2 - v_d^2) \right) \mathbf{1} \quad (\text{A5})$$

$$m_{RR}^2 = m_u^2 + \frac{v_u^2}{2} Y_u Y_u^\dagger + \frac{1}{24} \left((g_{BL}^2 + g_{BLR}^2 + 2(g_{BLR}g_R + g_{BL}g_{RBL}) - 3(g_R^2 + g_{RBL}^2)) (v_{\chi_R}^2 - v_{\bar{\chi}_R}^2) + (g_{BL}g_{RBL} + g_{BLR}g_R + 3(g_R^2 + g_{RBL}^2)) (v_d^2 - v_u^2) \right) \mathbf{1} \quad (\text{A6})$$

- **Mass of the Charged Higgs boson:** One obtains the same expression as in the MSSM:

$$m_{H^\pm}^2 = B_\mu (\tan \beta + \cot \beta) + m_W^2 \quad (\text{A7})$$

- **Mass matrix for Charginos, Basis:** $(\tilde{W}^-, \tilde{H}_d^-), (\tilde{W}^+, \tilde{H}_u^+)$

$$m_{\tilde{\chi}^\pm} = \begin{pmatrix} M_2 & \frac{1}{\sqrt{2}} g_L v_u \\ \frac{1}{\sqrt{2}} g_L v_d & \mu \end{pmatrix} \quad (\text{A8})$$

2. Calculation of the mass spectrum

We are going to present now the basic steps to calculate the mass spectrum. As starting point we use electroweak precision data to get the gauge and Yukawa couplings: the SM-like Yukawa couplings are calculated from the fermion masses and the one-loop relations of ref. [73] which have been adjusted to our model. Similarly, also the standard model gauge couplings are calculated by the same procedure presented in ref. [73], but again, including all new contributions of the mode under consideration. Since the entire RGE

running is performed in the basis $SU(3)_C \times SU(2)_L \times U(1)_R \times U(1)_{B-L}$, the value of the GUT normalized g_{BL} and g_R are matched to the GUT normalized hypercharge coupling g_Y by

$$g_R = c_{RY} g_Y, \quad (\text{A9})$$

$$g_{BL} = \frac{5g_{BLR}g_{RBL}g_R - \sqrt{6}g_{RBL}g_Y^2 + \sqrt{(3g_{BLR}^2 - 2\sqrt{6}g_{BLR}g_R + 2g_R^2)(5(g_R^2 + g_{RBL}^2 - 3g_Y^2)g_Y^2)}}{5g_R^2 - 3g_Y^2}. \quad (\text{A10})$$

This is nothing else than an inversion of the well known relation between the gauge couplings for $U(1)_R \times U(1)_{B-L} \rightarrow U(1)_Y$ including the off-diagonal gauge couplings given in eq. (A11). We are using the $SO(10)$ GUT normalization of $\sqrt{\frac{3}{5}}$ for $U(1)_Y$ and $\sqrt{\frac{3}{2}}$ for $U(1)_{B-L}$. To get the correct values of c_{RY} as well as g_{RBL} and g_{BLR} an iterative procedure is used: c_{RY} is calculated as ratio of the g_Y and g_{BL} when running down from the GUT scale and applying

$$g_Y = \sqrt{\frac{5(g_{BL}g_R - g_{BLR}g_{RBL})^2}{3(g_{BL}^2 + g_{BLR}^2) + 2(g_R^2 + g_{RBL}^2) - 2\sqrt{6}(g_Rg_{BLR} + g_{BL}g_{RBL})}} \quad (\text{A11})$$

When the gauge and Yukawa couplings are derived, the RGEs are then evaluated up to the GUT scale where the corresponding boundary conditions of eqs. (5), (6) and (12) are applied. Afterwards a RGE running of the full set of parameters to the SUSY scale is performed. We use always 2-loop RGEs which include the full effect of kinetic mixing [64, 117].

The running parameters are then used to calculate the tree level mass spectrum. However, it is well known that the one-loop corrections can be very important for particular particles and have to be taken into account. The best known example is the light MSSM Higgs boson which get shifted by up to 50% per-cent in case of heavy stops. Similar effects can be expected in the extended Higgs sector especially since these can be very light at tree-level. Similarly, the gauginos arising in an extended gauge sector can be potentially light and receive important corrections at one-loop [65]. To take these and all other possible effects into account we use a complete one-loop correction of the entire mass spectrum. Our procedure to calculate the one-loop masses is based on the method proposed in Ref.[73]: first, all running $\overline{\text{DR}}$ parameters are calculated at the SUSY scale and the SUSY masses at tree-level are derived. The EW vevs v_d and v_u are afterwards re-calculated using the one-loop corrected Z mass and demanding

$$m_Z^2 + \delta m_Z^2 = \frac{(g_{BL}^2 g_L^2 + g_{BL}^2 g_R^2 + g_L^2 g_R^2) v^2}{4(g_{BL}^2 + g_R^2)} (v_d^2 + v_u^2) \quad (\text{A12})$$

in addition with the running value of $\tan \beta$. Note that δm_Z^2 as well as all other self-energies include the corrections originated by all particles present in the mBLR. These calculations are performed in $\overline{\text{DR}}$ scheme and 't Hooft gauge. Also the complete dependence on the external momenta are taken into account. The re-calculated vevs are afterwards used to

solve the tree-level tadpole equations again and to re-calculate the tree-level mass spectrum as well as all vertices entering the one-loop corrections. Using these vertices and masses, the one-loop corrections δt_i to the tadpole equations are derived and we use as renormalization condition

$$t_i - \delta t_i = 0. \quad (\text{A13})$$

These one-loop corrected tadpole equations are solved with respect to the same parameter as at tree level resulting in new parameters $\mu^{(1)}, B_\mu^{(1)}, \mu_R^{(1)}, B_{\mu_R}^{(1)}$ respectively $\mu^{(1)}, B_\mu^{(1)}, m_{\chi_R}^{2,(1)}, m_{\bar{\chi}_R}^{2,(1)}$. The final step is to calculate all self-energies for different particles and to use those to get the one-loop corrected mass spectrum.

1. **Real scalars:** for a real scalar ϕ , the one-loop corrections are included by calculating the real part of the poles of the corresponding propagator matrices [73]

$$\text{Det} [p_i^2 \mathbf{1} - m_{\phi,1L}^2(p^2)] = 0, \quad (\text{A14})$$

where

$$m_{\phi,1L}^2(p^2) = \tilde{m}_{\phi,T}^2 - \Pi_\phi(p^2). \quad (\text{A15})$$

Equation (A14) has to be solved for each eigenvalue $p^2 = m_i^2$ which can be achieved in an iterative procedure. This has to be done also for charged scalars as well as the fermions. Note, \tilde{m}_T^2 is the tree-level mass matrix but for the parameters fixed by the tadpole equations the one-loop corrected values $X^{(1)}$ are used.

2. **Complex scalars:** for a complex scalar η field we use at one-loop level

$$m_{1L}^{2,\eta}(p_i^2) = \tilde{m}_T^{2,\eta} - \Pi_\eta(p_i^2), \quad (\text{A16})$$

While in case of sfermions $\tilde{m}_T^{2,\eta}$ agrees exactly with the tree-level mass matrix, for charged Higgs bosons $\mu^{(1)}$ and $B_\mu^{(1)}$ or $m_{H_d}^{(1)}$ and $m_{\bar{H}_d}^{(1)}$ has to be used depending on the set of parameters the tadpole equations are solved for.

3. **Majorana fermions:** the one-loop mass matrix of a Majorana χ fermion is related to the tree-level mass matrix by

$$M_{1L}^\chi(p_i^2) = M_T^\chi - \frac{1}{2} \left[\Sigma_S^0(p_i^2) + \Sigma_S^{0,T}(p_i^2) + \left(\Sigma_L^{0,T}(p_i^2) + \Sigma_R^0(p_i^2) \right) M_T^\chi + M_T^{\chi 0} \left(\Sigma_R^{0,T}(p_i^2) + \Sigma_L^0(p_i^2) \right) \right], \quad (\text{A17})$$

where we have denoted the wave-function corrections by Σ_R^0, Σ_L^0 and the direct one-loop contribution to the mass by Σ_S^0 .

4. **Dirac fermions:** for a Dirac fermion Ψ one has to add the self-energies as

$$M_{1L}^\Psi(p_i^2) = M_T^\Psi - \Sigma_S^+(p_i^2) - \Sigma_R^+(p_i^2) M_T^\Psi - M_T^\Psi \Sigma_L^+(p_i^2). \quad (\text{A18})$$

Note, this procedure agrees with the method implemented in `SPheno 3.1.10` to calculate the loop masses in the MSSM as well as with the code produced by `SARAH 3.0.39` or later. However, there are small differences to earlier versions of `SPheno` as well as other spectrum calculators: the MSSM equivalent of condition eq (A12) is often solved in an iterative way using the one-loop corrected parameters from the tadpole equations to calculate δm_Z^2 until $m_Z^2 + \delta m_Z^2$ has converged. In this context also $\mu^{(1)}$ and $B_\mu^{(1)}$ are used in the vertices entering the one-loop corrections. However, these steps mix tree- and one-loop level and break therefore gauge invariance: when we tried this approach the relation between Goldstone and gauge bosons mass is violated. However, the numerical differences in case of the MSSM turned out to be rather small.

As example we give the necessary formulae to calculate the one-loop corrections to the tadpole equations and the scalar Higgs masses in appendix A 3.

3. 1-loop corrections of the Higgs sector

As discussed in section A 2 we have calculated the entire mass spectrum at one-loop. For that purpose it is necessary to calculate all possible 1-loop diagrams for the one- and two-point functions. As example we here give the corresponding expressions for the one-loop corrections of the tadpoles as well as the self-energy for the scalar Higgs fields. For all other self-energies we refer to the output of `SARAH`¹¹. The results are expressed via Passarino Veltman integrals [73]. The basic integrals are

$$A_0(m) = 16\pi^2 Q^{4-n} \int \frac{d^n q}{i(2\pi)^n} \frac{1}{q^2 - m^2 + i\varepsilon}, \quad (\text{A19})$$

$$B_0(p, m_1, m_2) = 16\pi^2 Q^{4-n} \int \frac{d^n q}{i(2\pi)^n} \frac{1}{\left[q^2 - m_1^2 + i\varepsilon \right] \left[(q-p)^2 - m_2^2 + i\varepsilon \right]}, \quad (\text{A20})$$

with the renormalization scale Q . All the other, necessary functions can be expressed by A_0 and B_0 . For instance,

$$B_1(p, m_1, m_2) = \frac{1}{2p^2} \left[A_0(m_2) - A_0(m_1) + (p^2 + m_1^2 - m_2^2) B_0(p, m_1, m_2) \right], \quad (\text{A21})$$

and

$$F_0(p, m_1, m_2) = A_0(m_1) - 2A_0(m_2) - (2p^2 + 2m_1^2 - m_2^2) B_0(p, m_1, m_2), \quad (\text{A22})$$

$$G_0(p, m_1, m_2) = (p^2 - m_1^2 - m_2^2) B_0(p, m_1, m_2) - A_0(m_1) - A_0(m_2) \quad (\text{A23})$$

The numerical evaluation of all loop-integrals is performed by `SPheno`. With this conventions we can write the one-loop tadpoles as

$$\delta t_{\sigma_i}^{(1)} = + \frac{3}{2} A_0(m_Z^2) \Gamma_{\sigma_i, Z, Z} + \frac{3}{2} A_0(m_{Z_R}^2) \Gamma_{\sigma_i, Z_R, Z_R} + 3 A_0(m_{W^-}^2) \Gamma_{\sigma_i, W^+, W^-}$$

¹¹ To get the model files of the mBLR which is not yet part of the public version of `SARAH` please send a mail to the authors.

$$\begin{aligned}
& + 16A_0\left(m_{\nu_1}^2\right)\Gamma_{\sigma_i,\nu_1,\nu_1}m_{\nu_1}^2 - \sum_{a=1}^2 A_0\left(m_{H_a^-}^2\right)\Gamma_{\sigma_i,H_a^+,H_a^-} \\
& + 4\sum_{a=1}^2 A_0\left(m_{\tilde{\chi}_a^-}^2\right)\Gamma_{\sigma_i,\tilde{\chi}_a^+,\tilde{\chi}_a^-}m_{\tilde{\chi}_a^-}^2 + 12\sum_{a=1}^3 A_0\left(m_{d_a}^2\right)\Gamma_{\sigma_i,\bar{d}_a,d_a}m_{d_a}^2 \\
& + 4\sum_{a=1}^3 A_0\left(m_{e_a}^2\right)\Gamma_{\sigma_i,\bar{e}_a,e_a}m_{e_a}^2 + 12\sum_{a=1}^3 A_0\left(m_{u_a}^2\right)\Gamma_{\sigma_i,\bar{u}_a,u_a}m_{u_a}^2 \\
& - \frac{1}{2}\sum_{a=1}^4 A_0\left(m_{A_{0,a}}^2\right)\Gamma_{\sigma_i,A_{0,a},A_{0,a}} - \frac{1}{2}\sum_{a=1}^4 A_0\left(m_{h_a}^2\right)\Gamma_{\sigma_i,h_a,h_a} - 3\sum_{a=1}^6 A_0\left(m_{\bar{d}_a}^2\right)\Gamma_{\sigma_i,\bar{d}_a^*,\bar{d}_a} \\
& - \sum_{a=1}^6 A_0\left(m_{\bar{e}_a}^2\right)\Gamma_{\sigma_i,\bar{e}_a^*,\bar{e}_a} - 3\sum_{a=1}^6 A_0\left(m_{\bar{u}_a}^2\right)\Gamma_{\sigma_i,\bar{u}_a^*,\bar{u}_a} \\
& + 2\sum_{a=1}^7 A_0\left(m_{\tilde{\chi}_a^0}^2\right)\Gamma_{\sigma_i,\tilde{\chi}_a^0,\tilde{\chi}_a^0}m_{\tilde{\chi}_a^0}^2 - \sum_{a=1}^9 A_0\left(m_{\tilde{\nu}_a}^2\right)\Gamma_{\sigma_i,\tilde{\nu}_a^*,\tilde{\nu}_a} \\
& + 2\sum_{a=1}^9 A_0\left(m_{\nu_a}^2\right)\Gamma_{\sigma_i,\nu_a,\nu_a}m_{\nu_a}^2 \tag{A24}
\end{aligned}$$

with $\sigma_i = (\sigma_d, \sigma_u, \sigma_R, \bar{\sigma}_R)_i^T$. Γ_{xyz} denotes the vertex of the three particles x, y, z , while Γ_{wxyz} will be used for four-point interactions. For chiral couplings we use Γ^L as coefficient of the left and Γ^R as coefficient of the right polarization operator. For instance, $\Gamma_{\sigma_d,Z,Z}$ is the coupling of a pure down-type Higgs to a Z boson while $\Gamma_{\sigma_R,\tilde{\chi}_2^0,\tilde{\chi}_2^0}$ corresponds to the left-chiral part of the interaction of a R -Higgs to a neutralino of the second generation. The expressions for all vertices can be obtained with SARAH.

Using these conventions the self-energy for the scalar Higgs fields reads

$$\begin{aligned}
\Pi_{\sigma_i,\sigma_j}(p^2) &= \frac{7}{4}B_0\left(p^2, m_Z^2, m_Z^2\right)\Gamma_{\sigma_j,Z,Z}^*\Gamma_{\sigma_i,Z,Z} \\
& + \frac{7}{2}B_0\left(p^2, m_Z^2, m_{Z_R}^2\right)\Gamma_{\sigma_j,Z_R,Z}^*\Gamma_{\sigma_i,Z_R,Z} + \frac{7}{4}B_0\left(p^2, m_{Z_R}^2, m_{Z_R}^2\right)\Gamma_{\sigma_j,Z_R,Z_R}^*\Gamma_{\sigma_i,Z_R,Z_R} \\
& + \frac{7}{2}B_0\left(p^2, m_{W^-}^2, m_{W^-}^2\right)\Gamma_{\sigma_j,W^+,W^-}^*\Gamma_{\sigma_i,W^+,W^-} + 2A_0\left(m_Z^2\right)\Gamma_{\sigma_i,\sigma_i,Z,Z} + 2A_0\left(m_{Z_R}^2\right)\Gamma_{\sigma_i,\sigma_i,Z_R,Z_R} \\
& + 4A_0\left(m_{W^-}^2\right)\Gamma_{\sigma_i,\sigma_i,W^+,W^-} - \sum_{a=1}^2 A_0\left(m_{H_a^-}^2\right)\Gamma_{\sigma_i,\sigma_i,H_a^+,H_a^-} \\
& + \sum_{a=1}^2 \sum_{b=1}^2 B_0\left(p^2, m_{H_a^-}^2, m_{H_b^-}^2\right)\Gamma_{\sigma_j,H_a^+,H_b^-}^*\Gamma_{\sigma_i,H_a^+,H_b^-} \\
& - 2\sum_{a=1}^2 m_{\tilde{\chi}_a^+} \sum_{b=1}^2 B_0\left(p^2, m_{\tilde{\chi}_a^-}^2, m_{\tilde{\chi}_b^-}^2\right)m_{\tilde{\chi}_b^-} \left(\Gamma_{\sigma_j,\tilde{\chi}_a^+,\tilde{\chi}_b^-}^{L*}\Gamma_{\sigma_i,\tilde{\chi}_a^+,\tilde{\chi}_b^-}^R + \Gamma_{\sigma_j,\tilde{\chi}_a^+,\tilde{\chi}_b^-}^{R*}\Gamma_{\sigma_i,\tilde{\chi}_a^+,\tilde{\chi}_b^-}^L\right) \\
& + \sum_{a=1}^2 \sum_{b=1}^2 G_0\left(p^2, m_{\tilde{\chi}_a^-}^2, m_{\tilde{\chi}_b^-}^2\right)\left(\Gamma_{\sigma_j,\tilde{\chi}_a^+,\tilde{\chi}_b^-}^{L*}\Gamma_{\sigma_i,\tilde{\chi}_a^+,\tilde{\chi}_b^-}^L + \Gamma_{\sigma_j,\tilde{\chi}_a^+,\tilde{\chi}_b^-}^{R*}\Gamma_{\sigma_i,\tilde{\chi}_a^+,\tilde{\chi}_b^-}^R\right)
\end{aligned}$$

$$\begin{aligned}
& -6 \sum_{a=1}^3 m_{\bar{d}_a} \sum_{b=1}^3 B_0(p^2, m_{\bar{d}_a}^2, m_{\bar{d}_b}^2) m_{d_b} \left(\Gamma_{\sigma_j, \bar{d}_a, d_b}^{L*} \Gamma_{\sigma_i, \bar{d}_a, d_b}^R + \Gamma_{\sigma_j, \bar{d}_a, d_b}^{R*} \Gamma_{\sigma_i, \bar{d}_a, d_b}^L \right) \\
& + 3 \sum_{a=1}^3 \sum_{b=1}^3 G_0(p^2, m_{\bar{d}_a}^2, m_{\bar{d}_b}^2) \left(\Gamma_{\sigma_j, \bar{d}_a, d_b}^{L*} \Gamma_{\sigma_i, \bar{d}_a, d_b}^L + \Gamma_{\sigma_j, \bar{d}_a, d_b}^{R*} \Gamma_{\sigma_i, \bar{d}_a, d_b}^R \right) \\
& - 2 \sum_{a=1}^3 m_{\bar{e}_a} \sum_{b=1}^3 B_0(p^2, m_{\bar{e}_a}^2, m_{\bar{e}_b}^2) m_{e_b} \left(\Gamma_{\sigma_j, \bar{e}_a, e_b}^{L*} \Gamma_{\sigma_i, \bar{e}_a, e_b}^R + \Gamma_{\sigma_j, \bar{e}_a, e_b}^{R*} \Gamma_{\sigma_i, \bar{e}_a, e_b}^L \right) \\
& + \sum_{a=1}^3 \sum_{b=1}^3 G_0(p^2, m_{\bar{e}_a}^2, m_{\bar{e}_b}^2) \left(\Gamma_{\sigma_j, \bar{e}_a, e_b}^{L*} \Gamma_{\sigma_i, \bar{e}_a, e_b}^L + \Gamma_{\sigma_j, \bar{e}_a, e_b}^{R*} \Gamma_{\sigma_i, \bar{e}_a, e_b}^R \right) \\
& - 6 \sum_{a=1}^3 m_{\bar{u}_a} \sum_{b=1}^3 B_0(p^2, m_{\bar{u}_a}^2, m_{\bar{u}_b}^2) m_{u_b} \left(\Gamma_{\sigma_j, \bar{u}_a, u_b}^{L*} \Gamma_{\sigma_i, \bar{u}_a, u_b}^R + \Gamma_{\sigma_j, \bar{u}_a, u_b}^{R*} \Gamma_{\sigma_i, \bar{u}_a, u_b}^L \right) \\
& + 3 \sum_{a=1}^3 \sum_{b=1}^3 G_0(p^2, m_{\bar{u}_a}^2, m_{\bar{u}_b}^2) \left(\Gamma_{\sigma_j, \bar{u}_a, u_b}^{L*} \Gamma_{\sigma_i, \bar{u}_a, u_b}^L + \Gamma_{\sigma_j, \bar{u}_a, u_b}^{R*} \Gamma_{\sigma_i, \bar{u}_a, u_b}^R \right) \\
& - \frac{1}{2} \sum_{a=1}^4 A_0(m_{A_0, a}^2) \Gamma_{\sigma_i, \sigma_i, A_0, a, A_0, a} - \frac{1}{2} \sum_{a=1}^4 A_0(m_{h_a}^2) \Gamma_{\sigma_i, \sigma_i, h_a, h_a} \\
& + \frac{1}{2} \sum_{a=1}^4 \sum_{b=1}^4 B_0(p^2, m_{A_0, a}^2, m_{A_0, b}^2) \Gamma_{\sigma_j, A_0, a, A_0, b}^* \Gamma_{\sigma_i, A_0, a, A_0, b} \\
& + \frac{1}{2} \sum_{a=1}^4 \sum_{b=1}^4 B_0(p^2, m_{h_a}^2, m_{h_b}^2) \Gamma_{\sigma_j, h_a, h_b}^* \Gamma_{\sigma_i, h_a, h_b} - 3 \sum_{a=1}^6 A_0(m_{\bar{d}_a}^2) \Gamma_{\sigma_i, \sigma_i, \bar{d}_a^*, \bar{d}_a} \\
& - \sum_{a=1}^6 A_0(m_{\bar{e}_a}^2) \Gamma_{\sigma_i, \sigma_i, \bar{e}_a^*, \bar{e}_a} - 3 \sum_{a=1}^6 A_0(m_{\bar{u}_a}^2) \Gamma_{\sigma_i, \sigma_i, \bar{u}_a^*, \bar{u}_a} \\
& + 3 \sum_{a=1}^6 \sum_{b=1}^6 B_0(p^2, m_{\bar{d}_a}^2, m_{\bar{d}_b}^2) \Gamma_{\sigma_j, \bar{d}_a^*, \bar{d}_b}^* \Gamma_{\sigma_i, \bar{d}_a^*, \bar{d}_b} + \sum_{a=1}^6 \sum_{b=1}^6 B_0(p^2, m_{\bar{e}_a}^2, m_{\bar{e}_b}^2) \Gamma_{\sigma_j, \bar{e}_a^*, \bar{e}_b}^* \Gamma_{\sigma_i, \bar{e}_a^*, \bar{e}_b} \\
& + 3 \sum_{a=1}^6 \sum_{b=1}^6 B_0(p^2, m_{\bar{u}_a}^2, m_{\bar{u}_b}^2) \Gamma_{\sigma_j, \bar{u}_a^*, \bar{u}_b}^* \Gamma_{\sigma_i, \bar{u}_a^*, \bar{u}_b} \\
& - \sum_{a=1}^7 m_{\bar{\chi}_a^0} \sum_{b=1}^7 B_0(p^2, m_{\bar{\chi}_a^0}^2, m_{\bar{\chi}_b^0}^2) m_{\bar{\chi}_b^0} \left(\Gamma_{\sigma_j, \bar{\chi}_a^0, \bar{\chi}_b^0}^{L*} \Gamma_{\sigma_i, \bar{\chi}_a^0, \bar{\chi}_b^0}^R + \Gamma_{\sigma_j, \bar{\chi}_a^0, \bar{\chi}_b^0}^{R*} \Gamma_{\sigma_i, \bar{\chi}_a^0, \bar{\chi}_b^0}^L \right) \\
& + \frac{1}{2} \sum_{a=1}^7 \sum_{b=1}^7 G_0(p^2, m_{\bar{\chi}_a^0}^2, m_{\bar{\chi}_b^0}^2) \left(\Gamma_{\sigma_j, \bar{\chi}_a^0, \bar{\chi}_b^0}^{L*} \Gamma_{\sigma_i, \bar{\chi}_a^0, \bar{\chi}_b^0}^L + \Gamma_{\sigma_j, \bar{\chi}_a^0, \bar{\chi}_b^0}^{R*} \Gamma_{\sigma_i, \bar{\chi}_a^0, \bar{\chi}_b^0}^R \right) \\
& - \sum_{a=1}^9 A_0(m_{\bar{\nu}_a}^2) \Gamma_{\sigma_i, \sigma_i, \bar{\nu}_a^*, \bar{\nu}_a} + \sum_{a=1}^9 \sum_{b=1}^9 B_0(p^2, m_{\bar{\nu}_a}^2, m_{\bar{\nu}_b}^2) \Gamma_{\sigma_j, \bar{\nu}_a^*, \bar{\nu}_b}^* \Gamma_{\sigma_i, \bar{\nu}_a^*, \bar{\nu}_b} \\
& - \sum_{a=1}^9 m_{\nu_a} \sum_{b=1}^9 B_0(p^2, m_{\nu_a}^2, m_{\nu_b}^2) m_{\nu_b} \left(\Gamma_{\sigma_j, \nu_a, \nu_b}^{L*} \Gamma_{\sigma_i, \nu_a, \nu_b}^R + \Gamma_{\sigma_j, \nu_a, \nu_b}^{R*} \Gamma_{\sigma_i, \nu_a, \nu_b}^L \right)
\end{aligned}$$

$$\begin{aligned}
& + \frac{1}{2} \sum_{a=1}^9 \sum_{b=1}^9 G_0 \left(p^2, m_{\nu_a}^2, m_{\nu_b}^2 \right) \left(\Gamma_{\sigma_j, \nu_a, \nu_b}^{L*} \Gamma_{\sigma_i, \nu_a, \nu_b}^L + \Gamma_{\sigma_j, \nu_a, \nu_b}^{R*} \Gamma_{\sigma_i, \nu_a, \nu_b}^R \right) \\
& + 2 \sum_{b=1}^2 \Gamma_{\sigma_j, W^+, H_b^-}^* \Gamma_{\sigma_i, W^+, H_b^-} F_0 \left(p^2, m_{H_b^-}^2, m_{W^-}^2 \right) + \sum_{b=1}^4 \Gamma_{\sigma_j, \gamma, A_{0,b}}^* \Gamma_{\sigma_i, \gamma, A_{0,b}} F_0 \left(p^2, m_{A_{0,b}}^2, 0 \right) \\
& + \sum_{b=1}^4 \Gamma_{\sigma_j, Z, A_{0,b}}^* \Gamma_{\sigma_i, Z, A_{0,b}} F_0 \left(p^2, m_{A_{0,b}}^2, m_Z^2 \right) + \sum_{b=1}^4 \Gamma_{\sigma_j, Z_R, A_{0,b}}^* \Gamma_{\sigma_i, Z_R, A_{0,b}} F_0 \left(p^2, m_{A_{0,b}}^2, m_{Z_R}^2 \right)
\end{aligned} \tag{A25}$$

4. RGEs

The calculation of the renormalization group equations performed by SARAH is based on the generic expression of [117]. In addition, the results of [64] are used to include the effect of kinetic mixing.

The β functions for the parameters of a general superpotential written as

$$W(\phi) = \frac{1}{2} \mu^{ij} \phi_i \phi_j + \frac{1}{6} Y^{ijk} \phi_i \phi_j \phi_k \tag{A26}$$

can be easily obtained from the shown results for the anomalous dimensions by using the relations [118, 119]

$$\beta_Y^{ijk} = Y^{p(ij} \gamma_p^{k)}, \tag{A27}$$

$$\beta_\mu^{ij} = \mu^{p(i} \gamma_p^{j)}. \tag{A28}$$

For the results of the other parameters as well as for the two-loop results which we skip here because of their length we suggest to use the function `CalcRGEs[]` of SARAH.

a. Anomalous dimensions

$$\gamma_{\hat{q}}^{(1)} = \frac{1}{12} \left(12 \left(Y_d^\dagger Y_d + Y_u^\dagger Y_u \right) - \left(18g_L^2 + 32g_s^2 + g_{BL}^2 + g_{BLR}^2 \right) \mathbf{1} \right) \tag{A29}$$

$$\gamma_{\hat{l}}^{(1)} = -\frac{3}{4} \left(2g_L^2 + g_{BL}^2 + g_{BLR}^2 \right) \mathbf{1} + Y_e^\dagger Y_e + Y_\nu^\dagger Y_\nu \tag{A30}$$

$$\gamma_{\hat{H}_d}^{(1)} = \frac{1}{2} \left(2\text{Tr} \left(Y_e Y_e^\dagger \right) - 3g_L^2 + 6\text{Tr} \left(Y_d Y_d^\dagger \right) - g_R^2 - g_{RBL}^2 \right) \tag{A31}$$

$$\gamma_{\hat{H}_u}^{(1)} = \frac{1}{2} \left(2\text{Tr} \left(Y_\nu Y_\nu^\dagger \right) - 3g_L^2 + 6\text{Tr} \left(Y_u Y_u^\dagger \right) - g_R^2 - g_{RBL}^2 \right) \tag{A32}$$

$$\gamma_{\hat{\chi}_R}^{(1)} = \frac{1}{4} \left(-2g_R^2 - 2g_{RBL}^2 + 2\sqrt{6}g_{BL}g_{RBL} + 2\sqrt{6}g_{BLR}g_R - 3g_{BL}^2 - 3g_{BLR}^2 + 4\text{Tr} \left(Y_s Y_s^\dagger \right) \right) \tag{A33}$$

$$\gamma_{\hat{\chi}_R}^{(1)} = \frac{1}{4} \left(-2(g_R^2 + g_{RBL}^2) + 2\sqrt{6}g_{BL}g_{RBL} + 2\sqrt{6}g_{BLR}g_R - 3g_{BL}^2 - 3g_{BLR}^2 \right) \quad (\text{A34})$$

$$\gamma_{\hat{S}}^{(1)} = Y_s^\dagger Y_s \quad (\text{A35})$$

$$\gamma_{\hat{u}}^{(1)} = \frac{1}{12} \left(24Y_u^* Y_u^T - \left(2\sqrt{6}g_{BL}g_{RBL} + 2\sqrt{6}g_{BLR}g_R + 32g_s^2 + 6g_R^2 + 6g_{RBL}^2 + g_{BL}^2 + g_{BLR}^2 \right) \mathbf{1} \right) \quad (\text{A36})$$

$$\gamma_{\hat{d}}^{(1)} = \frac{1}{12} \left(24Y_d^* Y_d^T - \left(-2\sqrt{6}g_{BL}g_{RBL} - 2\sqrt{6}g_{BLR}g_R + 32g_s^2 + 6g_R^2 + 6g_{RBL}^2 + g_{BL}^2 + g_{BLR}^2 \right) \mathbf{1} \right) \quad (\text{A37})$$

$$\gamma_{\hat{\nu}}^{(1)} = \frac{1}{4} \left(- \left(2(g_R^2 + g_{RBL}^2) - 2\sqrt{6}g_{BL}g_{RBL} - 2\sqrt{6}g_{BLR}g_R + 3g_{BL}^2 + 3g_{BLR}^2 \right) \mathbf{1} + 4 \left(2Y_v^* Y_v^T + Y_s^* Y_s^T \right) \right) \quad (\text{A38})$$

$$\gamma_{\hat{e}}^{(1)} = \frac{1}{4} \left(- \left(2(g_R^2 + g_{RBL}^2) + 2\sqrt{6}g_{BL}g_{RBL} + 2\sqrt{6}g_{BLR}g_R + 3g_{BL}^2 + 3g_{BLR}^2 \right) \mathbf{1} + 8Y_e^* Y_e^T \right) \quad (\text{A39})$$

b. Gauge Couplings

$$\beta_{g_{BL}}^{(1)} = \frac{1}{4} \left(27g_{BL}^3 - 2\sqrt{6}g_{BL}^2 g_{RBL} + g_{BL} \left(27g_{BLR}^2 + 30g_{RBL}^2 - \sqrt{6}g_{BLR}g_R \right) + g_{BLR} \left(30g_R - \sqrt{6}g_{BLR} \right) g_{RBL} \right) \quad (\text{A40})$$

$$\beta_{g_R}^{(1)} = \frac{1}{4} \left(27g_{BL}g_{BLR}g_{RBL} + 27g_{BLR}^2 g_R - 2\sqrt{6}g_{BLR}g_R^2 + 30g_R^3 + 30g_Rg_{RBL}^2 - \sqrt{6}g_{BL}g_Rg_{RBL} - \sqrt{6}g_{BLR}g_{RBL}^2 \right) \quad (\text{A41})$$

$$\beta_{g_{BLR}}^{(1)} = \frac{1}{4} \left(g_{BL}^2 \left(27g_{BLR} - \sqrt{6}g_R \right) + g_{BL} \left(30g_Rg_{RBL} - \sqrt{6}g_{BLR}g_{RBL} \right) + g_{BLR} \left(27g_{BLR}^2 - 2\sqrt{6}g_{BLR}g_R + 30g_R^2 \right) \right) \quad (\text{A42})$$

$$\beta_{g_{RBL}}^{(1)} = \frac{1}{4} \left(27g_{BL}^2 g_{RBL} + 30g_{RBL} \left(g_R^2 + g_{RBL}^2 \right) + g_{BL} \left(27g_{BLR}g_R - \sqrt{6} \left(2g_{RBL}^2 + g_R^2 \right) \right) - \sqrt{6}g_{BLR}g_Rg_{RBL} \right) \quad (\text{A43})$$

$$\beta_{g_L}^{(1)} = g_L^3 \quad (\text{A44})$$

$$\beta_{g_s}^{(1)} = -3g_s^3 \quad (\text{A45})$$

c. *Gaugino Mass Parameters*

$$\beta_{M_{BL}}^{(1)} = \frac{1}{2} \left(27g_{BL}^2 M_{BL} - g_{BL} \left(-27g_{BLR} M_{BR} + 2\sqrt{6}g_{RBL} M_{BL} + \sqrt{6}g_R M_{BR} \right) + g_{RBL} \left(30g_{RBL} M_{BL} + 30g_R M_{BR} - \sqrt{6}g_{BLR} M_{BR} \right) \right) \quad (\text{A46})$$

$$\beta_{M_R}^{(1)} = \frac{1}{2} \left(27g_{BLR}^2 M_R + 30g_R \left(g_{RBL} M_{BR} + g_R M_R \right) + g_{BL} \left(27g_{BLR} - \sqrt{6}g_R \right) M_{BR} - \sqrt{6}g_{BLR} \left(2g_R M_R + g_{RBL} M_{BR} \right) \right) \quad (\text{A47})$$

$$\beta_{M_{BR}}^{(1)} = \frac{1}{4} \left(27g_{BL}^2 M_{BR} + 27g_{BLR}^2 M_{BR} - \sqrt{6}g_{BLR} \left(2g_R M_{BR} + g_{RBL} \left(M_{BL} + M_R \right) \right) + 30 \left(g_R^2 M_{BR} + g_{RBL}^2 M_{BR} + g_R g_{RBL} \left(M_{BL} + M_R \right) \right) + g_{BL} \left(27g_{BLR} \left(M_{BL} + M_R \right) - \sqrt{6} \left(2g_{RBL} M_{BR} + g_R \left(M_{BL} + M_R \right) \right) \right) \right) \quad (\text{A48})$$

$$\beta_{M_2}^{(1)} = 2g_L^2 M_2 \quad (\text{A49})$$

$$\beta_{M_3}^{(1)} = -6g_s^2 M_3 \quad (\text{A50})$$

- [1] M. Malinsky, J. C. Romao and J. W. F. Valle, Phys. Rev. Lett. **95** (2005) 161801 [arXiv:hep-ph/0506296].
- [2] V. De Romeri, M. Hirsch, M. Malinsky, Phys. Rev. **D84** 053012 (2011); [arXiv:1107.3412 [hep-ph]].
- [3] R. Mohapatra and J. Valle, Phys. Rev. **D34**, 1642 (1986).
- [4] E. K. Akhmedov, M. Lindner, E. Schnapka and J. W. F. Valle, Phys. Rev. D **53**, 2752 (1996) [hep-ph/9509255].
- [5] E. K. Akhmedov, M. Lindner, E. Schnapka and J. W. F. Valle, Phys. Lett. B **368**, 270 (1996) [hep-ph/9507275].
- [6] M. Hirsch, M. Malinsky, W. Porod, L. Reichert and F. Staub, JHEP **1202**, 084 (2012) [arXiv:1110.3037 [hep-ph]].
- [7] ATLAS Collaboration, G. Aad et al., Phys.Lett. **B710**, 49 (2012), arXiv:1202.1408.
- [8] CMS Collaboration, S. Chatrchyan et al., (2012), arXiv:1202.1488.
- [9] L. J. Hall, D. Pinner and J. T. Ruderman, arXiv:1112.2703 [hep-ph].
- [10] H. Baer, V. Barger and A. Mustafayev, arXiv:1112.3017 [hep-ph].
- [11] J. L. Feng, K. T. Matchev and D. Sanford, arXiv:1112.3021 [hep-ph].
- [12] S. Heinemeyer, O. Stal and G. Weiglein, arXiv:1112.3026 [hep-ph].
- [13] A. Arbey, M. Battaglia, A. Djouadi, F. Mahmoudi and J. Quevillon, Phys. Lett. B **708** (2012) 162 [arXiv:1112.3028 [hep-ph]].

- [14] A. Arbey, M. Battaglia and F. Mahmoudi, Eur. Phys. J. C **72** (2012) 1906 [arXiv:1112.3032 [hep-ph]].
- [15] P. Draper, P. Meade, M. Reece and D. Shih, arXiv:1112.3068 [hep-ph].
- [16] T. Moroi, R. Sato and T. T. Yanagida, Phys. Lett. B **709** (2012) 218 [arXiv:1112.3142 [hep-ph]].
- [17] M. Carena, S. Gori, N. R. Shah and C. E. M. Wagner, arXiv:1112.3336 [hep-ph].
- [18] U. Ellwanger, arXiv:1112.3548 [hep-ph].
- [19] O. Buchmueller, *et al.*, arXiv:1112.3564 [hep-ph].
- [20] S. Akula, B. Altunkaynak, D. Feldman, P. Nath and G. Peim, arXiv:1112.3645 [hep-ph].
- [21] M. Kadastik, K. Kannike, A. Racioppi and M. Raidal, arXiv:1112.3647 [hep-ph].
- [22] J. Cao, Z. Heng, D. Li and J. M. Yang, arXiv:1112.4391 [hep-ph].
- [23] A. Arvanitaki and G. Villadoro, arXiv:1112.4835 [hep-ph].
- [24] M. Gozdz, arXiv:1201.0875 [hep-ph].
- [25] J. F. Gunion, Y. Jiang and S. Kraml, arXiv:1201.0982 [hep-ph].
- [26] G. G. Ross and K. Schmidt-Hoberg, arXiv:1108.1284 [hep-ph].
- [27] G. G. Ross, K. Schmidt-Hoberg and F. Staub, arXiv:1205.1509 [hep-ph].
- [28] P. Fileviez Perez, arXiv:1201.1501 [hep-ph].
- [29] N. Karagiannakis, G. Lazarides and C. Pallis, arXiv:1201.2111 [hep-ph].
- [30] S. F. King, M. Muhlleitner and R. Nevzorov, arXiv:1201.2671 [hep-ph].
- [31] Z. Kang, J. Li and T. Li, arXiv:1201.5305 [hep-ph].
- [32] C. -F. Chang, K. Cheung, Y. -C. Lin and T. -C. Yuan, arXiv:1202.0054 [hep-ph].
- [33] L. Aparicio, D. G. Cerdeno and L. E. Ibanez, arXiv:1202.0822 [hep-ph].
- [34] L. Roszkowski, E. M. Sessolo and Y. -L. S. Tsai, arXiv:1202.1503 [hep-ph].
- [35] J. Ellis and K. A. Olive, arXiv:1202.3262 [hep-ph].
- [36] H. Baer, V. Barger and A. Mustafayev, arXiv:1202.4038 [hep-ph].
- [37] N. Desai, B. Mukhopadhyaya and S. Niyogi, arXiv:1202.5190 [hep-ph].
- [38] J. Cao, Z. Heng, J. M. Yang, Y. Zhang and J. Zhu, arXiv:1202.5821 [hep-ph].
- [39] L. Maiani, A. D. Polosa and V. Riquer, arXiv:1202.5998 [hep-ph].
- [40] T. Cheng, J. Li, T. Li, D. V. Nanopoulos and C. Tong, arXiv:1202.6088 [hep-ph].
- [41] N. Christensen, T. Han and S. Su, arXiv:1203.3207 [hep-ph].
- [42] D. A. Vasquez, G. Belanger, C. Boehm, J. Da Silva, P. Richardson and C. Wymant, arXiv:1203.3446 [hep-ph].
- [43] U. Ellwanger and C. Hugonie, arXiv:1203.5048 [hep-ph].
- [44] Updated results can be found on the web-page: <https://twiki.cern.ch/twiki/bin/view/AtlasPublic>; see, especially: ATLAS-CONF-2012-033
- [45] Updated results can be found on the web-page: <https://twiki.cern.ch/twiki/bin/view/CMSPublic/PhysicsResults>
- [46] H. E. Haber, M. Sher, Phys. Rev. **D35** (1987) 2206.
- [47] M. Drees, Phys. Rev. **D35** (1987) 2910-2913.
- [48] M. Cvetič, D. A. Demir, J. R. Espinosa, L. L. Everett, P. Langacker, Phys. Rev. **D56** (1997)

2861. [hep-ph/9703317].
- [49] Y. Zhang, H. An, X. d. Ji and R. N. Mohapatra, Phys. Rev. D **78**, 011302 (2008) [arXiv:0804.0268 [hep-ph]].
 - [50] E. Ma, [arXiv:1108.4029 [hep-ph]].
 - [51] K. Nakamura *et al.* [Particle Data Group Collaboration], J. Phys. G **37**, 075021 (2010).
 - [52] T. Falk, K. A. Olive and M. Srednicki, Phys. Lett. B **339**, 248 (1994) [hep-ph/9409270].
 - [53] A. Ali, D. A. Demir, M. Frank and I. Turan, Phys. Rev. D **79** (2009) 095001 [arXiv:0902.3826 [hep-ph]].
 - [54] A. Belyaev, J. P. Hall, S. F. King and P. Svantesson, arXiv:1203.2495 [hep-ph].
 - [55] Mohapatra, Rabindra N., Phys. Rev. D **34**, 3457 (1986).
 - [56] Aulakh, Charanjit S. and Benakli, Karim and Senjanović, Goran, Phys. Lett. **79**, 2188 (1997).
 - [57] S. P. Martin, Phys. Rev. D **46**, 2769 (1992) [hep-ph/9207218].
 - [58] C.S. Aulakh and R.N. Mohapatra, Phys. Lett. B **119**, 136 (1982).
 - [59] Mitsuo J. Hayashi and Akihiro Murayama, Phys. Lett. B **153**, 251 (1985).
 - [60] Mohapatra, Rabindra N., Phys. Rev. Lett. **56**, 561 (1986).
 - [61] B. C. Allanach *et al.*, Comput. Phys. Commun. **180** (2009) 8-25. [arXiv:0801.0045 [hep-ph]].
 - [62] B. Holdom, Phys. Lett. B **166**, 196 (1986).
 - [63] K. S. Babu, C. F. Kolda and J. March-Russell, Phys. Rev. D **57** (1998) 6788 [arXiv:hep-ph/9710441].
 - [64] R. Fonseca, M. Malinsky, W. Porod, F. Staub, Nucl. Phys. **B854** (2012) 28-53. [arXiv:1107.2670 [hep-ph]].
 - [65] B. O'Leary, W. Porod and F. Staub, JHEP **1205** (2012) 042 [arXiv:1112.4600 [hep-ph]].
 - [66] F. Braam and J. Reuter, arXiv:1107.2806 [hep-ph].
 - [67] E. J. Chun, J. -C. Park and S. Scopel, JHEP **1102** (2011) 100 [arXiv:1011.3300 [hep-ph]].
 - [68] Y. Mambrini, JCAP **1107**, 009 (2011) [arXiv:1104.4799 [hep-ph]].
 - [69] T. G. Rizzo, Phys. Rev. D **85**, 055010 (2012) [arXiv:1201.2898 [hep-ph]].
 - [70] D. Matalliotakis and H. P. Nilles, Nucl. Phys. B **435**, 115 (1995) [hep-ph/9407251].
 - [71] N. Polonsky and A. Pomarol, Phys. Rev. D **51**, 6532 (1995) [hep-ph/9410231].
 - [72] V. Berezhinsky, A. Bottino, J. R. Ellis, N. Fornengo, G. Mignola and S. Scopel, Astropart. Phys. **5**, 1 (1996) [hep-ph/9508249].
 - [73] D. M. Pierce, J. A. Bagger, K. T. Matchev, R. -j. Zhang, Nucl. Phys. **B491** (1997) 3-67. [hep-ph/9606211].
 - [74] W. Porod, Comput. Phys. Commun. **153** (2003) 275 [arXiv:hep-ph/0301101].
 - [75] W. Porod and F. Staub, arXiv:1104.1573 [hep-ph].
 - [76] F. Staub, arXiv:0806.0538 [hep-ph].
 - [77] F. Staub, arXiv:0909.2863 [hep-ph].
 - [78] F. Staub, Comput. Phys. Commun. **182** (2011) 808 [arXiv:1002.0840 [hep-ph]].
 - [79] ATLAS conference note ATLAS-CONF-2012-007, see [44]
 - [80] J. Erler, P. Langacker, S. Munir, E. Rojas, [arXiv:1103.2659 [hep-ph]].
 - [81] Tomas G. Rizzo, [arXiv:0610104 [hep-ph]].

- [82] J. Beringer et al. (Particle Data Group), Phys. Rev. D **86** (2012) 010001
- [83] M. Hirsch, H. V. Klapdor-Kleingrothaus and S. G. Kovalenko, Phys. Lett. B **398**, 311 (1997) [hep-ph/9701253].
- [84] M. Hirsch, J. W. F. Valle, W. Porod, J. C. Romao and A. Villanova del Moral, Phys. Rev. D **78** (2008) 013006 [arXiv:0804.4072 [hep-ph]].
- [85] M. Hirsch, S. Kaneko and W. Porod, Phys. Rev. D **78**, 093004 (2008) [arXiv:0806.3361 [hep-ph]].
- [86] J. N. Esteves, J. C. Romao, M. Hirsch, F. Staub and W. Porod, Phys. Rev. D **83**, 013003 (2011) [arXiv:1010.6000 [hep-ph]].
- [87] M. Hirsch, F. Staub and A. Vicente, arXiv:1202.1825 [hep-ph].
- [88] J. Adam *et al.* [MEG collaboration], Phys. Rev. Lett. **107** (2011) 171801 [arXiv:1107.5547 [hep-ex]].
- [89] P. Bechtle, O. Brein, S. Heinemeyer, G. Weiglein and K. E. Williams, Comput. Phys. Commun. **181** (2010) 138 [arXiv:0811.4169 [hep-ph]].
- [90] P. Bechtle, O. Brein, S. Heinemeyer, G. Weiglein and K. E. Williams, arXiv:1102.1898 [hep-ph].
- [91] G. Degrossi, P. Slavich and F. Zwirner, Nucl. Phys. B **611** (2001) 403.
- [92] A. Brignole, G. Degrossi, P. Slavich and F. Zwirner, Nucl. Phys. B **631** (2002) 195.
- [93] A. Brignole, G. Degrossi, P. Slavich and F. Zwirner, Nucl. Phys. B **643** (2002) 79.
- [94] A. Dedes and P. Slavich, Nucl. Phys. B **657** (2003) 333.
- [95] A. Dedes, G. Degrossi and P. Slavich, Nucl. Phys. B **672** (2003) 144.
- [96] B. C. Allanach, A. Djouadi, J. L. Kneur, W. Porod and P. Slavich, JHEP **0409** (2004) 044 [hep-ph/0406166].
- [97] A. Nisati, for the ATLAS collaboration, talk presented at Lepton-Photon Conference 2011, Mumbai, India, August 2011.
- [98] V. Sharma, for the CMS collaboration, talk presented at Lepton-Photon Conference 2011, Mumbai, India, August 2011.
- [99] E. Etzion, private communication.
- [100] EChang, Chun-Fu and Cheung, Kingman and Yuan, Tzu-Chiang, JHEP **09** (2011) 58 [arXiv:1107.1133 [hep-ph]].
- [101] G. Aad *et al.* [ATLAS Collaboration], Phys. Rev. Lett. **107** (2011) 272002 [arXiv:1108.1582 [hep-ex]].
- [102] S. Chatrchyan *et al.* [CMS Collaboration], JHEP **1105** (2011) 093 [arXiv:1103.0981 [hep-ex]].
- [103] W. Kilian, T. Ohl and J. Reuter, Eur. Phys. J. C **71**, 1742 (2011) [arXiv:0708.4233 [hep-ph]].
- [104] M. Moretti, T. Ohl and J. Reuter, arXiv:hep-ph/0102195.
- [105] F. Staub, T. Ohl, W. Porod, C. Speckner, [arXiv:1109.5147 [hep-ph]].
- [106] B. Fuks, M. Klasen, F. Ledroit, Q. Li and J. Morel, Nucl. Phys. B **797** (2008) 322 [arXiv:0711.0749 [hep-ph]].
- [107] F. del Aguila, J. A. Aguilar-Saavedra and R. Pittau, JHEP **0710** (2007) 047 [hep-ph/0703261].

- [108] J. A. Aguilar-Saavedra, Nucl. Phys. B **828** (2010) 289 [arXiv:0905.2221 [hep-ph]].
- [109] S. P. Das, F. F. Deppisch, O. Kittel and J. W. F. Valle, arXiv:1206.0256 [hep-ph].
- [110] S. Gopalakrishna, A. de Gouvea and W. Porod, JCAP **0605** (2006) 005 [hep-ph/0602027].
- [111] C. Arina and N. Fornengo, JHEP **0711** (2007) 029 [arXiv:0709.4477 [hep-ph]].
- [112] Z. Thomas, D. Tucker-Smith and N. Weiner, Phys. Rev. D **77** (2008) 115015 [arXiv:0712.4146 [hep-ph]].
- [113] D. G. Cerdeno, C. Munoz and O. Seto, Phys. Rev. D **79** (2009) 023510 [arXiv:0807.3029 [hep-ph]].
- [114] P. Bandyopadhyay, E. J. Chun and J. -C. Park, JHEP **1106** (2011) 129 [arXiv:1105.1652 [hep-ph]].
- [115] G. Belanger, J. Da Silva and A. Pukhov, JCAP **1112** (2011) 014 [arXiv:1110.2414 [hep-ph]].
- [116] B. Dumont, G. Belanger, S. Fichet, S. Kraml and T. Schwetz, arXiv:1206.1521 [hep-ph].
- [117] S. P. Martin and M. T. Vaughn, Phys. Rev. D **50** (1994) 2282 [Erratum-ibid. D **78** (2008) 039903] [arXiv:hep-ph/9311340].
- [118] P. C. West, Phys. Lett. B **137** (1984) 371.
- [119] D. R. T. Jones and L. Mezincescu, Phys. Lett. B **138**, 293 (1984).